Swansea University

MSc by research

Theoretical Physics

# Renormalisation group flows and holography in lower dimensions

*Author:*

Sam Mulligan

*Supervisors:*

Professor Maurizio Piai

Professor Daniel Thompson

March 7, 2025

**Abstract**

In this thesis, we study renormalisation group flows of special strongly coupled field theories in dimensions lower than four using their gravity dual description in four dimensions. Starting from a particular four-dimensional bosonic theory truncated from eleven-dimensional supergravity described by Gauntlett et al[1], we perform our own further consistent truncation down to two scalars coupled to gravity. In doing so we are able to identify new classical solutions to maximally supersymmetric supergravity in four dimensions. The solutions we find fall into two broad classes, those for which the dual field theories are conformal at long distances, and those that confine in the same limit. We discuss their global stability properties by studying the holographically renormalised free energy. We find that the confining branch of solutions are stable and energetically favoured compared to conformal solutions in the equivalent portion of the parameter space.

# Declaration of Authorship

I, Sam Mulligan, declare that this thesis, entitled renormalisation group flows and holography in lower dimensions, and the work presented within are my own, and has been composed and generated solely by myself in a program of original research for the degree of MSc by research at Swansea university. This work was completed wholly while in candidature for the aforementioned degree and university and no part of this thesis has previously been submitted for any other degree or qualification at this or any other institution. Any work that is not my own original research and has been quoted or drawn from the published work of others has been clearly attributed and the sources are clearly given in the attached bibliography. In all cases, the university's ethical procedures have been followed and good research practice has been observed. Where appropriate, ethical approval has been granted. I hereby give consent for my thesis, if accepted to be available for electronic sharing.

With the following signature, I hereby declare all the above to be truthful to the best of my understanding.

Signed: 

Date: 07/03/2025

# Acknowledgements

First and foremost, I would like to thank my supervisors Maurizio and Daniel for helping to shape and further my understanding of theoretical physics, and preparing me to navigate the challenges of the world of academia. Throughout my time in Swansea, Maurizio in particular has been a constant source of guidance, support and insight, helping me to deal with all my questions and challenges with patience, understanding and humour. I would also like to thank the new friends and colleagues I have made here in swansea who, most being much more experienced than I, have helped greatly to soften the learning curve on a topic I was very much new too. I thank also my old friends from my time in southampton, who are now doing physics of their own up and down the country, for the helpful advice about my work, and for keeping life enjoyable when things started to become difficult. Finally, I would like to thank my parents and family for their constant moral, financial, practical, and emotional support and encouragement, without which this thesis would have been impossible.

# Contents

# 1 Introduction

As work has continued in the field of high energy physics in the past few decades, it has become increasingly clear that the standard model must be modified or replaced by a more complete theory at some new energy scale $\Lambda$. Continuing investigations at the LHC and elsewhere have failed to find convincing evidence of new physics, resulting in the most conservative lower bounds of $\Lambda$ being well into the TeV range.

If, however, new physics at these scales play any role in electroweak symmetry breaking, it would seem to be incompatible with the relatively low observed mass of the Higgs boson [2, 3] without explicit fine tuning. As a possible solution, it has been suggested that if it is possible to tune the effects of explicit breaking of scale invariance to be less than the effects of spontaneous symmetry breaking, the Higgs may in fact be what is known as a dilaton[4, 5], the boson associated with spontaneous symmetry breaking, allowing the Higgs mass to be low enough to match experimentally observed values without explicit fine tuning[6, 7, 8, 9].

This approach does not come without its limitations, as it is particularly difficult computationally to develop effective field theory descriptions of the dilaton when we are starting from the point of view of a strongly coupled field theory. An alternative approach utilising the $AdS$/CFT correspondence therefore has begun to be utilised to great effect.[10, 11]

First introduced by Maldacena [12] in 1997, the $AdS$/CFT correspondence [13] has proven to be a tremendously powerful tool for studying strongly coupled quantum field theories (QFTs), and is, thus far, the most successful realization of the earlier proposed holographic principle of quantum gravity [14]. In the most general terms, this holographic principles provides us with a method of computing field-theory observables indirectly, by instead studying a so-called dual gravity theory in a curved spacetime. Working within such a gravity theory, we can take the boundary values of objects within the bulk geometry, such as strings and fields, and arrive at a description perfectly equivalent to the corresponding quantum field theory. The usefullness of this approach lies in the fact that, for a strongly interacting field theory, the fields in the equivalent gravitational theory are, in fact, weakly interacting, making the problem much more mathematically tractable.

The $AdS$/CFT correspondence has found success in the analysis of a number of real world physical systems, such as condensed matter physics [15], the study of exotic states of matter including superfluids and superconducters, and quantum chromodynamics (QCD), which describes the interaction of quarks and gluons via the strong force. Provided that the field theory in question is consistent, then we should expect that their dual gravity description is itself a consistent theory, with examples including string theory or M-theory.

A lack of divergences or need for renormalisation means string theory remains an attractive prospect as theory of quantum gravity. Regardless, a number of its core assumptions, such as the replacement of particles and fields with one-dimensional strings, are difficult to verify experimentally and raise questions about whether the theory is empirically sound. As a direct supersymmetric extension to general relativity, supergravity in its maximally symmetric form circumvents some of these problems by retaining point particles and fields, making fewer assumptions and being conceptually simple compared to string theory. As a toy model, its potential for ultraviolet finiteness and insights into the perturbative structure of quantum gravity make it a useful test bed for studying alternative models of quantum gravity and extensions to the standard model by acting as a low energy approximation of string theory.

In this thesis, we will primarily consider a very well known approach to quantum gravity known as supergravity (SUGRA). More specifically, we concern ourselves with a particular dimensional reduction of 11-dimensional SUGRA, $N = 8$ supergravity in four dimensions. It is well known that classical supergravity represents the gauge theory limit of string theory and M-theory for large numbers of colours, $N_C \to \infty$, and strong coupling, $\lambda \to \infty$. Upon first glance, this may appear to present a problem, as quantum chromodynamics is neither strongly coupled at all energy scales, nor does it contain a large number of colours. However, while the dual field theory description for supergravity may not describe the 'real world' as it were, it is still of great interest of us to search for gauge theory descriptions, dual to supergravity, that nevertheless share some properties with real world models such as QCD, with the hope that perhaps some of the results we obtain within the former theories are also applicable to the latter.

In the course of this investigation our work will be based on a broad program of research outlined in [16] which uses a number of ideas first applied within a "bottom up" approach to holography [17, 18, 19], applying them however in the context of a more rigorous "top-down" approach such as in [20], in which we will take a known supergravity theory and adjust the boundary conditions satisfied by its constituent scalar fields at the end of space, corresponding to far-UV in its holographic dual. As described in [21], our investigation works within the confines of a theory in which the spacial geometry is asymptotically Anti-de Sitter as we approach the boundary of the space at infinity.

As the supergravity theory under consideration is weakly coupled, our starting point for this investigation will be to find the fixed point solutions using the classical equations of motion derived from the action, and represent critical points in the potential of the system. From here, we will go on to calculate numerical solutions which flow between these points. Under the gauge-gravity duality, these fixed point solutions correspond to different conformal field theories in one fewer dimension. Crucially, this means that our interpolating numerical solutions in fact represent renormalisation group flows between two theories at different energy scales, one in the Ultraviolet (UV), and the other, Infrared (IR).

A renormalisation group (RG) flow describes a running of the couplings in a renormalizable quantum field theory when we view the system at differing scales. As such, we can learn a great deal about the nature of a given system by studying its RG flow, and in particular allow us to analyse the free energy of a given class of interpolating solutions defined by a family of parameters in the IR.

Previous studies [22, 23, 16] suggest that by analysing the mass spectrum of the theory, one may be able to identify a point in the parameter space where the field excitations have negative mass squared, and the field is said to be tachyonic. In this case, the potential associated with the field is an unstable maximum in which scale invariance may become spontaneously broken as the field rolls to a new vacuum. Fluctuations of the scalar field in the vicinity this instability can hence be identified as an (approximate) dilaton. Thus, if one finds a tachyonic instability in the theory for a given class of solutions, then an investigation of the spectra in its vicinity

may reveal the existence of a scalar that is both parametrically light and an approximate dilaton.[22]

We can compare the relative stability between varying classes of solution to the classical equations of motion by analysing the free energy density of the gravity background as a function of the parameter space characterising the 'UV' region of the background. It is this process which will form the primary results of this thesis. By comparing different classes of solution, it is possible to observe if there exists a phase transition[19, 24] which prevents us from dialing the UV boundary parameters to have arbitrarily small mass due to the massless dilaton state existing on a now unstable branch of solutions.

In Section 2 of this thesis, we outline the theoretical background of gauge gravity dualities and holographic renormalisation, followed In section 3 by a description of the supergravity background we will be studying, the details of consistent truncation of the supergravity action, and then extracting the equations of motion from the resulting action. Finally, we solve these equations for a background which is asymptotically $AdS$ at both ends of the space, first analytically for fixed point vacuum solutions and then again numerically for solutions which interpolate between these points. In section 4, we will then consider backgrounds where the space in our dual gravity description closes off smoothly at the one boundary, and one of the circular coordinates which defines the geometry shrinks to zero size after performing a double analytic continuation. Finally, in section 5 we will compare the behaviour of the free energy between the two different branches of solution we have discussed, first the IR solutions, followed by those that confine.

In doing so, we hope to develop a clear picture of the energetics of our chosen gravity background in order to pave the way for future studies of the mass spectra of the theory, such that if an approximate dilation exists along either of these solutions, it will be clear if such a solution is stable or merely metastable in the relevant region of the parameter space.

# 2 Background and Formalism

In this section, we will briefly outline the theoretical background required for an understanding of the main body of work. In particular, we will broadly define much of the language of conformal field theories, supergravities, $AdS$ spaces, which will be important for making formal statement of the gauge-gravity duality, a core concept used throughout this thesis.

## 2.1 Conformal field theories

As one might expect, a key step in understanding the nature of the $AdS$/CFT correspondence is to first define what we mean by a conformal field theory (CFT). In quantum field theory, one often encounters scale invariance as a natural symmetry due to the implicit scale invariance of fixed points in the renormalisation group. A CFT, however, exhibits a stronger form of this invariance that is not necessarily found in nature without additional assumptions [25]. A field theory exhibiting conformal invariance, simply put, is invariant under *conformal transformations*. A conformal transformation is any transformation in which the lengths of vectors are altered but the angles between them are preserved. In more concrete terms, if we perform some coordinate transform such that $x \to x'$, it is a conformal transformation if the metric is transformed by some scale factor $\Omega(x)$ [26]:

$$g_{\mu\nu}(x) \to g'_{\mu\nu}(x') = \Omega(x) g_{\mu\nu}(x) \tag{1}$$

With a flat minkowski metric $g_{\mu\nu} = \eta_{\mu\nu}$, this leads to a set of three possible conformal transformations and symmetry groups. First, the standard Lorentz and Poincaré invariance,

$$x^\mu \to x'^\mu = x^\mu + a^\mu, \qquad \Omega = 1, \tag{2}$$

$$x^\mu \to x'^\mu = \Lambda^\mu_\nu x^\mu, \tag{3}$$

followed by invariance under transformations of scale, or *dilatations*

$$x^\mu \to x'^\mu = \lambda x^\mu, \qquad \Omega = \lambda^{-1}, \tag{4}$$

and finally, special conformal transformations of the form

$$x^\mu \to x'^\mu = \frac{x^\mu + b^\mu x^\mu x_\mu}{1 + 2b^\mu x_\mu + b^\mu b_\mu x^\mu x_\mu}, \qquad \Omega(x) = (1 + 2b^\mu x_\mu + b^\mu b_\mu x^\mu x_\mu)^2. \tag{5}$$

In other words, in a four-dimensional spacetime our conformal transformation group consists of four translations, three rotations, three Lorentz boosts, 1 dilatation, and 4 special conformal transformations. This gives fifteen generators that form the conformal group $SO(6)$

## 2.2 Gauge-gravity dualities

We are presented with two very different scientific paradigms; conformal field theories, existing in our regular minkowski space, and some gravitational theory embedded on a space whose geometry is at least asymptotically Anti-de Sitter. Yet we find that these two descriptions are deeply connected in a surprising but mathematically elegant way. In this section, we will provide a brief overview of the gauge-gravity duality, outline the formalism of holographic renormalisation, and precisely defining in quantitative terms the correspondence between supergravity in $AdS$ space and conformal field theories on the boundary.

Let us posit the existence of a scalar dilaton field $\Phi$ in a bulk volume that is asymptotically $AdS_{d+1}$, for which we impose the boundary condition that $\Phi$ approaches some given function $\phi_0$ at infinity. As such, the on-shell bulk partition function, identified at the boundary, is given by

$$Z_{SUGRA}[\phi_0] = \int_{\Phi \sim \phi_0} D\Phi \exp(-S[\Phi]). \tag{6}$$

Now, let us consider the case of a conformal field theory defined by a set of n point correlation functions $\langle \mathcal{O}(x_1)\mathcal{O}(x_2)...\mathcal{O}(x_n)\rangle$ which we might hope to compute. Assuming that the composite field operator $\mathcal{O}$ is coupled to a source field $J(x)$ with coupling $\int_{S^d} J(x)\mathcal{O}(x)$

on $AdS_d$, then the partition function of the quantum field theory is given by

$$Z_{CFT}[J] = \int D\psi \exp\left(-S[\psi(x)] + \int d^d x J(x)\mathcal{O}(x)\right) = \langle \exp\left(\int d^d x J(x)\mathcal{O}(x)\right)\rangle. \tag{7}$$

From this generating functional one hopes to be able to evaluate the complete set of connected n point correlation functions

$$\langle \mathcal{O}(x_1)\mathcal{O}(x_2)...\mathcal{O}(x_n)\rangle = (-1)^n \left.\frac{\delta^n W_{CFT}[J]}{\delta J(x_1)\dots\delta J(x_n)}\right|_{J=0}, \tag{8}$$

where $W_{CFT}[J] = -\ln Z[J]$

Associating the source field $J(x)$ of the operator $\mathcal{O}$ to the boundary dilaton value in $AdS_{d+!}$ leads us to the core conceit of the gauge gravity duality. Specifically, that

$$Z_{SUGRA}[\phi_0] = \int_{\Phi\sim\phi_0} D\Phi \exp(-S[\Phi]) = \langle \exp\left(-\int d^d x \phi_0 \mathcal{O}(x)\right)\rangle. \tag{9}$$

We can see that while the right hand side of this equation represents the generating functional for a strongly coupled CFT, the partition function on the left hand side satisfies all the properties of a *weakly* coupled field theory. As such one need not (and indeed cannot) directly evaluate the connected correlation functions from the QFT partition function, and instead may simply solve the classical equations of motion derived from the on-shell action $S[\phi_0]$. The relation above thereby becomes

$$S_{onshell}[\phi_0] = -W_{CFT}[\phi_0], \tag{10}$$

and the correlation functions of the operator $\mathcal{O}$ can therefore be defined in terms of derivatives of the on-shell action,

$$\langle \mathcal{O}(x_1)\mathcal{O}(x_2)...\mathcal{O}(x_n)\rangle = (-1)^{n+1} \left.\frac{\delta^n S_{onshell}[\phi_0]}{\delta\phi_0(x_1)\dots\delta\phi_0(x_n)}\right|_{\phi_0=0}, \tag{11}$$

However, in the absence of proper renormalisation, for strongly coupled cases such as this,

the QFT correlation functions diverge and the generating function W is ill-defined. To make matters worse, the supergravity action on the right hand side also diverges as the bulk space we are integrating over has infinite volume. In order to compute exact n-point correlation functions one must first take the appropriate steps of holographic renormalisation.

After a process of renormalisation, we can define exact 1 point correlation functions $\langle \mathcal{O}(x) \rangle$ for each bulk field $\phi$ that can be simply determined by an asymptotic analysis of the field equations.

## 2.3 Renormalisation group flows

Given an arbitrary $D = d + 1$ dimensional gravity theory with a well defined Lagrangian, in general it is sufficient for holographic computations to use solutions derived from the Poincare invariant half space metric,

$$ds^2 = d\rho^2 + e^{2\mathcal{A}(\rho)} dx_\mu dx^\mu, \tag{12}$$

where $dx_\mu dx^\mu$ is interpreted as either $d$-dimensional Euclidean, or $d$-dimensional Minkowski spacetime. For simplicity, we choose to work with a metric in which the ordinary Minkowski metric has been substituted for a four-dimensional Euclidean metric by way of what is known as a Wick rotation [27]. This metric is asymptotically $AdS$, and in particular we recover $AdS$ solutions for $\mathcal{A}(\rho) \sim \rho / R_{AdS}$.

Starting then with a general four-dimensional action containing only scalar fields

$$\mathcal{S} = \int d^D x \sqrt{-g} \left[ \frac{\mathcal{R}}{4} - \frac{1}{2} G_{ab} g^{MN} \partial_M \Phi^a \partial_N \Phi^b - V(\Phi^a) \right], \tag{13}$$

it follows that if the scalars have only a dependence on the radial coordinate $\rho$, then the effective equations of motion are given by

$$\partial_\rho^2 \Phi^a + (D-1) \partial_\rho \mathcal{A} \partial_\rho \Phi^a + \mathcal{G}^a_{bc} \partial_\rho \Phi^b \partial_\rho \Phi^c - G^{ab} \partial_b V = 0, \tag{14}$$

and the Einstein equations are

$$(D-1)(\partial_\rho \mathcal{A})^2 + \partial_\rho^2 \mathcal{A} + \frac{4}{D-2} V = 0, \tag{15}$$

$$(D-1)(D-2)(\partial_\rho \mathcal{A})^2 - 2G_{ab}\partial_\rho \Phi^a \partial_\rho \Phi^b + 4V = 0. \tag{16}$$

The first and most immediate solutions to these equations are the so-called 'fixed point' boundary solutions obtained at local critical points of the potential V for which $\frac{\partial V}{\phi_0^a} = 0$, where $\phi_0^a$ is taken to be the value of the field $\Phi^a$ at the boundary. From the Einstein equations we can also extract the $AdS$ curvature by noting that on the boundary we will have solutions $\mathcal{A}(\rho) \sim \rho / R_{AdS}$ and so $V_{min} = -(D-1)(D-2)/4R_{AdS}^2$

At this point however, as we are only considering solutions which are asymptotically $AdS$ we will find it useful for future calculations to introduce an appropriate change of coordinates $z = R_{AdS} e^{-\mathcal{A}(\rho)}$ such that the metric is written in Poincare coordinates

$$ds^2 = \frac{R_{AdS}^2}{z^2}\left(dz^2 + dx_\mu dx^\mu\right). \tag{17}$$

Taking the limit $z \to 0$, this metric is conformally equivalent to the Minkowski/Euclidean metric. As such, we take these fixed point boundary solutions to be dual to some Conformal field theory which lives in the conformal Minkowski/Euclidean space at infinity.

Now, assuming the equations of motion for Scalar field $\Phi^a$ have some boundary solution $\phi^a = \phi_0$, then we can construct more general solutions by performing a near-boundary expansion about the $AdS$ vacuum. For small $z$, the field behaviour in the asymptotic limit will depend on boundary condition $\phi_0$ and parameters $\phi_1$ and $\phi_2$ as

$$\phi^a(z) = \phi_0 + z^{d-\Delta}\phi_1 + \cdots + z^\Delta \phi_2 + \ldots, \tag{18}$$

where the quantity $\Delta$ is interpreted as the scaling dimension of the operator $O$ in the dual theory. The scaling dimension is related to the masses of the masses $m_a^2$ of the scalar fields and the $AdS$ curvature in a well known result, where

$$\Delta = \frac{d}{2} + \sqrt{\frac{d^2}{4} + m^2 R_{AdS}^2} \tag{19}$$

$$\Delta(\Delta - d) = m^2 R_{AdS}^2. \tag{20}$$

In the standard language of the $AdS$/CFT correspondance, we interpret $\phi_1$ as the source field for some dual operator $\mathcal{O}$, while we associate $\phi_2$ with the one-point function of the dual operator. It follows then that, given a supergravity solution in an asymptotically $AdS$ spacetime, we may interpret non-boundary bulk solutions in two different ways. In the case that our solution is asymptotic to $z^{d-\Delta}$, we treat the expansion as an operator deformation of the original CFT, corresponding to the addition of a term $\int d^d x \phi_1 O$ to the Lagrangian. Conversely, if our near-boundary expansion is proportional to $z^{\Delta}$, then the Lagrangian remains the same as the boundary CFT, but the operator acquires a non-zero VEV deformation and solutions become associated with a different, non-conformally invariant vacuum $\sim \phi_2$

In the holographic dual, altering the $CFT$ in this way and thereby breaking the conformal invariance induces a running of the couplings with some energy scale. Our bulk gravitational solutions are therefore said to correspond to a renormalisation group (RG) flow between two different quantum field theory vacua. We may associate this energy scale as increasing with the radial coordinate $\rho$, placing the ultraviolet (UV) region at $\rho \to \infty$, while the functions describing the bulk scalar fields encode how the parameters change with said scale.

A particularly intriguing scenario occurs when our supergravity potential V permits another critical point where the value of the scalar field $\phi(\rho) = \phi_{IR}$ is non-zero. In this case a UV CFT under some relevant deformation will experience an RG flow to another fixed point in the Infrared (IR). The IR fixed point is represented in the dual by solutions which asymptote towards the opposite $AdS$ boundary to the UV fixed point. Explicitly, this means that $\mathcal{A} \to \rho/R_{IR}$ for $\rho \to -\infty$, and $\mathcal{A} \to \rho/R_{UV}$ for $\rho \to +\infty$. The exploration of this concept represents the core of the body of this thesis.

## 2.4 Holographic renormalisation

We have shown that, given a classical gravity background, one can use the classical action to construct on-shell equations of motion that can be solved to obtain a scalar $\phi$. Despite this, as mentioned earlier in this chapter, our results cannot possibly permit a dual field theory interpretation unless the classical action is appropriately renormalised.

Having obtained a general solution to the field equations of motion in the asymptotic limit of the form given in equations (14)-(16), we would find constructing the bulk action $\mathcal{S}$ in terms of local functions of the source field $\phi_0$, $\phi_1$, and $\phi_2$ leaves terms that diverge as the coordinate $z \to 0$. Removing these divergent terms is entailed by the process of *holographic renormalisation*, in which the bulk action must be supplemented with extra terms to enforce the proper field dynamic at the boundary.

On the question of whether the addition of terms to the action is well motivated, we note that such additions are not just allowed, but in fact required by the presence of boundaries. Without the addition of a Gibbons-Hawking-York(GHY) term for example, the variational principle is ill defined, leading to inconsistencies when attempting to define the equations of motion and Einstein equations.[28, 29].

Once we have a regularised on-shell action $\mathcal{S}_{reg}$, the divergent terms may be isolated and removed by adding a boundary-localized potential counter-term action $\mathcal{S}_{ct}$ which is also written in terms of an asymptotic expansion. The renormalised action is thus simply the limit of the sum of these two terms, i.e,

$$\mathcal{S}_{ren} = \lim_{z \to 0} \left( \mathcal{S}_{reg} + \mathcal{S}_{ct} \right). \tag{21}$$

A more thorough treatment of this process of renormalisation can be found in [30, 31, 32], for our purposes, we merely state that once we have obtained the renormalised action, we automatically obtain the exact 1 point functions of the dual operator $\mathcal{O}$ in the presence of sources as

$$\langle \mathcal{O} \rangle = \frac{1}{\sqrt{g}} \frac{\delta S_{ren}}{\delta \phi_0} \sim \phi_2. \tag{22}$$

If the one-point function is known exactly, then the n-point correlation functions can be solved by differentiating and setting the sources to zero.

$$\langle \mathcal{O}(x_1)...\mathcal{O}(x_n)\rangle = \frac{\delta\phi_2}{\delta\phi_0(x_2)...\delta\phi_0(x_n)}\bigg|_{\phi_0=0}. \tag{23}$$

# 3 The Supergravity theory

## 3.1 Strings, Superstrings, and M theory

Before discussing our primary focus of the gravity side of the gauge-gravity duality, supergravity, we first familiarise ourselves with the closely related world of string theory, superstring theory, and M theory. String theories were first devised in order to model the strong interaction. While this was ultimately abandoned in favour of the enduring and succesful theory of quantum chromodynamics, the properties that made it unsuitable to describe the strong force made it an attractive prospect as a theory of quantum gravity. Subsequently, the five known consistent superstring theories (type I, type IIA, type IIB, and two versions of heterotic string theory) were conjectured to be merely limiting cases of a greater, 11-dimensional theory known as M theory [33, 34]. This discovery was vital to the development of the gauge/gravity duality, as the first definitive examples of the $AdS$/CFT correspondence were formulated from M-theory. [12]

The principle objects of study in string theory are $1+1$ dimensional objects known as strings. The many different particles in the standard model reduce to different quantized vibrational modes of these strings. Unlike the standard model, however, these fluctuations also contain a state corresponding to a massless spin-2 field, or graviton, making string theory a theory of quantum gravity.

Returning to the concept of M-theory, it was observed that in the limit of strong coupling, type IIA string theory appears to be identical to an 11-dimensional theory compactified on a circle with radius proportional to the strength of the coupling[33, 35, 34]. This 11-dimensional theory is M-theory. In the low energy limit of this theory, we may consider only the massless

string modes as the massive modes have decoupled, leaving us with 11-dimensional Supergravity (11-D SUGRA). This 11-D SUGRA will be the fundamental theory on which the analysis in this thesis is based.

## 3.2 11-D SUGRA, compactification and consistent truncation

We start with a $D = 11$ supergravity that is the product of an $AdS_{d+1}$ space and some internal space $M$. The generalized Lagrangian for such a space is given by

$$\mathcal{L} = \sqrt{g}(\frac{R}{4} - \frac{1}{48}F_{\mu\nu\gamma\sigma}F^{\mu\nu\gamma\sigma}) + \frac{1}{72}A \wedge F \wedge, F + fermions \tag{24}$$

where $A$ is a 3-form gauge field and $F = dA$ [13]. To derive the field content of such a theory, it must first be *compactified* to a lower number of dimensions. This means that we must define the space of the higher dimensional theory as the product of a $d+1$ dimensional spacetime with a compact $D-d-1$ internal manifold $M$, in which the size of the 'extra' $D-d-1$ dimensions are small relative to the $d+1$ dimensional space. A natural compactification was found by Freund and Rubin [36], in which the theory can be reduced to 4 or 7 dimensions.

Once the space has been compactified, deriving the field content of the 11-dimensional theory requires performing a *consistent Kaluza-Klein truncation*. Typically, fields in the full 11-dimensional theory can be represented as an infinite series of Kaluza-Klein (KK) modes. For example, a scalar field $\Phi(x, y)$, where $x$ are the co-ordiates of the lower dimensional space and $y$ are co-ordinates on the internal space $M$, can be expanded as

$$\Phi(x, y) = \sum_{n}^{\infty} \phi_n(x) Y_n(y), \tag{25}$$

in the higher dimensional theory, where $\phi_n(x)$ are the KK modes, and $Y_n(y)$ are eigenfunctions on $M$. However, at low energies, higher modes corresponding to higher energy states are suppressed. As such, in constructing a lower dimensional effective field theory description, we can truncate the full series expansion and keep only a finite number of modes that characterise the field behaviour at low energies. If solutions to the equations of motion of the truncated

theory lift to solutions to the equivalent equations of motion of the higher dimensional theory, then the truncation is said to be consistent.

It has been conjectured [37] that for any supersymmetric solution of this larger dimensional theory, there exists a consistent KK truncation on $M$ such that we obtain a supergravity theory in $d+1$ dimensions that contains only fields which are dual to the fields in the current multiplet of a super-conformal field theory. For a number of general cases, this conjecture has been shown to be true. [38, 39, 40, 41]

In this investigation we restrict our attention to the known compactification of $D = 11$ supergravity on a seven-dimensional Sasaki-Einstein ($SE_7$) space, which may be truncated to obtain $N = 2$ supergravity in $D = 4$. For the special case of $SE_7 = S^7$, $S^7$ being the seven-sphere, it has additionally been demonstrated that there exists a general consistent truncation to $N = 8$ supergravity in four dimensions [42]. While there exist a number of four-dimensional compactifications of 11-dimensional supergravity, a review of which can be found in [43], we will use an ansatz defined by an explicit KK reduction that is constructed only for a small number of bosonic fields. It has been shown in [44, 45] that if a consistent truncation can be constructed containing only the bosonic fields, then the supersymmetry of the higher dimensional theory dictates that an extension of the reduction to the fermionic sector is also consistent.

## 3.3 Maximally gauged supergravity

As previously stated, we study a supergravity reduction on a $AdS_4 \times SE_7$ space, where $SE_7$ is a seven-dimensional *Sasaki-Einstein* manifold that is compactified relative to the $AdS$ space. Our interest in this particular compactification is well motivated by the well-substantiated result that truncations of this four-dimensional theory exhibit $\mathcal{N} = 1, 2, 4$ and 8 supersymmetry, depending on the specific choice of $SE_7$ manifold [13].

The most intriguing of these cases is the reduction of $S^7$ to obtain a supergravity that exhibits local $SO(8) \times SU(8)$ invariance. Hence, to fully place our investigation in context, we provide a brief overview of $N = 8$ supergravity and its significance.

In four dimensions the maximal supergroup corresponding to a supergravity theory is $OSp(8|4)$. Hence, the largest extended supergravity model is built upon a single irreducible multiplet of $N = 8$ supersymmetry, containing maximal spin 2 and in which a graviton is coupled naturally with particles of lower spin. This is what we will refer to as the maximally supersymmetric supergravity model throughout this thesis.

Our supermultiplet of massless physical states consists of the aforementioned spin 2 graviton, as well as eight spin $\frac{3}{2}$ gravitinos. We also have 28 spin 1 gravi-photons, 56 spin $\frac{1}{2}$ gravi-spinors and 70 spin 0 scalar states. Each of these fields displays different behaviour under complex internal symmetry groups, with the graviton behaving as a singlet in all cases, and the fermions being associated with 8 and 56-dimensional chiral $SU(8)$ representations. The 28 vector fields, however, are unable to permit transformations under internal symmetry, the largest invariance group allowed being $SO(8)$

It is possible to construct a complete description of $N = 8$ supergravity [46] by using its $E_7 \times SU(8)$ structure to facilitate the construction of transformation rules and a complete Lagrangian, and also utilising the lowest order results referenced in [47]. Thus, it is not necessary to prove that the full N=8 supergravity action is indeed invariant under supersymmetric transformations, as the construction used in [46] relies on the reduction of 11-dimensional supergravity, which has been completely established to be invariant, allowing the four-dimensional theory to follow unambiguously.

We find that a truncation of the aforementioned $D = 11$ theory removes all dependence on the internal $S^7$ space from the 11-dimensional equations of motion, and we may derive said equations of motion from the four-dimensional action. As such, this truncation has been shown to correspond to vacuum solutions of the potential for scalar fields in $\mathcal{N} = 8$ supergravity. [48]

One of the most exciting, and perhaps primary, results of string theory, is that it doesn't lead to divergences and as such does not require renormalisation. If it can be shown that $N = 8$ supergravity shares this property of finiteness, then string theory is no longer unique, and it may be the case that there are other ways of handling divergences which do not lead to many of the additional more troublesome predictions or assumptions of string theory. At

present, the four loop amplitude of $N = 8$ supergravity has been shown to be ultraviolet finite in both four and five dimensions [49, 50]. If this behaviour remains unbroken at the, admittedly difficult to calculate, level of seven loops then it suggests that the theory may indeed be perturbatively finite at all orders. Maximally symmetric supergravity, then, may form a crucial foundation for studying more physically realistic models by capturing many of the essential features of string theory without having to concern ourselves with the staggering complexity of string dynamics.

## 3.4 Compactification and truncation on $AdS \times SE_7$

The supersymmetric class of $AdS_4 \times SE_7$ solutions of D=11 supergravity are given by the metric and four form field strength respectively,

$$\begin{aligned} ds^2 &= \frac{1}{4} ds^2(AdS_4) + ds^2(SE_7), \\ G_4 &= \frac{3}{8} vol(AdS_4). \end{aligned} \tag{26}$$

A full construction of the ansatz used in the compactification of the $D = 11$ theory, as well as the form of the four-dimensional action is given in [1] and does not need to be repeated here. It suffices to say, however, that using the ansatz in [1] defining the consistent truncation, we find that there is no longer any dependence on the $SE_7$ space in the $D = 11$ equations of motion. As such, if one finds a solution to the equations of motion for the $D = 4$ metric g and a collection of matter fields, then one also has a solution to the full $D = 11$ supergravity equations of motion.

The four-dimensional action used in [1], from which one may derive $D = 4$ equations of motion and which contains only bosonic modes, in fact permits a further consistent truncation to just the scalar fields and the metric. Equations of motions for the scalar fields follow from

the four-dimensional action

$$\mathcal{S} = \int d^4x\sqrt{-g}\left[R_E - 42(\nabla u)^2 - \frac{7}{2}(\nabla v)^2 - \frac{3}{2}e^{-8u-2v}(\nabla h)^2 - \frac{3}{2}e^{6u-2v}(\nabla\chi_R)^2 \right.$$
$$\left. +48e^{2u-3v} - 6e^{16u-3v} - 24h^2e^{8u-5v} - 18(\epsilon + h^2 + \chi_R^2)e^{-7v} - 24e^{-6u-5v}\chi_R^2\right] \quad (27)$$

where $u, v, h$ are scalar fields, $\chi_R$ is the real part of the scalar field $\chi$, g is the determinant of the metric and $R_E$ is the Ricci scalar. We can identify the scalar fields u and v as the "squashing mode" and "breathing mode" which act together to preserve the volume of the $SE_7$ space. We take note of the constant $\epsilon = \pm 1$ which defines the extent to which our compactified solutions preserve the supersymmetry present in the higher dimensional theory. When $\epsilon = 1$, solutions uplifted to $AdS \times SE_7$ will generally preserve at least $N = 2$ supersymmetry. Conversely, solutions with $\epsilon = -1$ are referred to as "skew-whiffed", in that supersymmetry has been broken during the process of compactification to the lower dimensional theory [51]. When $SE_7 = S^7$ however, the vacuum of the theory for both classes of solution will preserve maximal $N = 8$ supersymmetry.

Using the prescription set forth in Section 2.3, the equations of motion for this particular truncation are

$$\partial_\rho^2 u + \frac{12}{7}\chi(\rho)^2 e^{-6u(\rho)-5v(\rho)} - \frac{16}{7}h(\rho)^2 e^{8u(\rho)-5v(\rho)} + 3\partial_\rho A\partial_\rho u - \frac{3}{28}(\partial_\rho\chi)^2 e^{6u(\rho)-2v(\rho)}$$
$$+\frac{1}{7}(\partial_\rho h)^2 e^{-8u(\rho)-2v(\rho)} + \frac{8}{7}e^{2u(\rho)-3v(\rho)} - \frac{8}{7}e^{16u(\rho)-3v(\rho)} = 0, \quad (28)$$

$$\partial_\rho^2 v + 36\chi(\rho)^2 h(\rho)^2 e^{-7v(\rho)} + \frac{120}{7}\chi(\rho)^2 e^{-6u(\rho)-5v(\rho)} + 18\chi(\rho)^4 e^{-7v(\rho)} - 36\chi(\rho)^2 e^{-7v(\rho)}$$
$$+\frac{120}{7}h(\rho)^2 e^{8u(\rho)-5v(\rho)} + 18h(\rho)^4 e^{-7v(\rho)} - 36h(\rho)^2 e^{-7v(\rho)} + 3\partial_\rho A\partial_\rho v + \frac{3}{7}(\partial_\rho\chi)^2 e^{6u(\rho)-2v(\rho)}$$
$$+\frac{3}{7}(\partial_\rho h)^2 e^{-8u(\rho)-2v(\rho)} - \frac{144}{7}e^{2u(\rho)-3v(\rho)} + \frac{18}{7}e^{16u(\rho)-3v(\rho)} + 18e^{-7v(\rho)} = 0, \quad (29)$$

$$\partial_\rho^2 h - 24\chi(\rho)^2 h(\rho) e^{8u(\rho)-5v(\rho)} - 24h(\rho)^3 e^{8u(\rho)-5v(\rho)} + 24h(\rho)e^{8u(\rho)-5v(\rho)}$$
$$-16h(\rho)e^{16u(\rho)-3v(\rho)} + 3\partial_\rho A \partial_\rho h - 8\partial_\rho h \partial_\rho u - 2\partial_\rho h \partial_\rho v = 0, \tag{30}$$

$$\partial_\rho^2 \chi - 24\chi(\rho) h(\rho)^2 e^{-6u(\rho)-5v(\rho)} - 24\chi(\rho)^3 e^{-6u(\rho)-5v(\rho)} + 24\chi(\rho)e^{-6u(\rho)-5v(\rho)}$$
$$-16\chi(\rho)e^{-12u(\rho)-3v(\rho)} + 3\partial_\rho A \partial_\rho \chi + 6\partial_\rho \chi \partial_\rho u - 2\partial_\rho \chi \partial_\rho v = 0, \tag{31}$$

### 3.5 A further consistent truncation

Starting from the action given in Equation (27), we perform the following change of variables defined in [1]. This first step diagonalises the terms in the action involving the scalar fields $U$ and $V$.[1]:

$$U = -u + \frac{1}{3}v, \tag{32}$$
$$V = 6u + \frac{1}{3}v, \tag{33}$$

which can be rearranged as

$$u = \frac{1}{7}(V - U), \tag{34}$$
$$v = \frac{1}{7}(18U + 3V). \tag{35}$$

When $\epsilon = -1$ we may introduce the further truncations [52]:

$$e^{6U} = 1 - \frac{3}{4}|\chi_R|^2, \tag{36}$$
$$e^{6V} = \frac{(1-h^2)^3}{(1-\frac{3}{4}|\chi_R|^2)^2}, \tag{37}$$

which, again, we can rearrange in the form

$$U = \frac{1}{6}\log[1 - \frac{3}{4}|\chi_R|^2], \tag{38}$$

$$V = \frac{1}{6}\log[\frac{(1-h^2)^3}{(1-\frac{3}{4}|\chi_R|^2)^2}]. \tag{39}$$

Finally, we can redefine $h$ and $\chi_R$ in terms of the new scalars $\phi$ and $\varphi$

$$h = \frac{e^{2\phi}-1}{e^{2\phi}+1}, \tag{40}$$

$$\chi_R = \frac{2}{\sqrt{3}}\frac{e^{2\varphi}-1}{e^{\varphi}+1}, \tag{41}$$

which leads us to arrive finally at the truncated four-dimensional action

$$\mathcal{S} = \int d^4x\sqrt{g}\left[\frac{R}{4} - \frac{3}{8}(\partial_\rho\phi)^2 - \frac{1}{2}(\partial_\rho\varphi)^2 + 6\cosh(\phi)\cosh^2(\varphi) - \frac{1}{2}\cosh(3\phi)\sinh^2(2\varphi)\right]. \tag{42}$$

## 3.6 Equations of Motion

After our action is truncated, our model permits a number of possible gravity backgrounds. As per the ansatz given by Equation (12), we consider only backgrounds in which one of the coordinates is parameterised by the holographic coordinate $\rho$. In particular, we explicitly choose backgrounds for which $\mathcal{A} = \mathcal{A}(\rho)$ so as to ensure the preservation of Poincare invariance. Using the general forms given in section 3.2, and given that

$$G_{ab} = \begin{pmatrix} \frac{3}{4} & 0 \\ 0 & 1 \end{pmatrix}, \tag{43}$$

$$G^{ab} = \begin{pmatrix} \frac{4}{3} & 0 \\ 0 & 1 \end{pmatrix}, \tag{44}$$

, our equations of motion are given by

$$\partial_\rho^2\phi + 3\partial_\rho\mathcal{A}(\rho)\partial_\rho\phi(\rho) - 2\sinh(3\phi(\rho))\sinh^2(2\varphi(\rho)) + 8\sinh(\phi(\rho))\cosh^2(\varphi(\rho)) = 0, \tag{45}$$

$$\partial_\rho^2\varphi + 3\partial_\rho\mathcal{A}(\rho)\partial_\rho\varphi(\rho) + 6\cosh(\phi(\rho))\sinh(2\varphi(\rho)) - \cosh(3\phi(\rho))\sinh(4\varphi(\rho)) = 0, \tag{46}$$

$$\partial_\rho^2\mathcal{A} + 3(\partial_\rho\mathcal{A})^2 - 12\cosh(\phi(\rho))\cosh(\varphi(\rho))^2 + \cosh(3\phi(\rho))\sinh(2\varphi(\rho)^2 = 0, \tag{47}$$

$$6(\partial_\rho\mathcal{A})^2 - \frac{6}{4}(\partial_\rho\phi)^2 - 2(\partial_\rho\varphi)^2 - 24\cosh(\phi(\rho))\cosh(\varphi(\rho))^2 + 2\cosh(3\phi(\rho))\sinh(2\varphi(\rho))^2 = 0. \tag{48}$$

## 3.7 AdS$_4$ vacuum solutions

We start with solutions that satisfy the critical points of the potential and have constant $\phi, \varphi$ and $\partial_\rho\mathcal{A}$. From the perspective of the gauge-gravity duality, these points are representative of the vacuum of a conformal field theory. A *very* detailed summary of the known critical points of $SO(8)$ supergravity and their properties can be found in [53]

In this section we will give the scaling dimensions of the boundary CFT's and we use equations (19)-(20) to give the masses of the scalar fields $\phi$ and $\varphi$. While we record the values pf $\Delta$ now, we note that they were obtained during a part of the investigation that we will deal with shortly, namely the asymptotic expansion of $\phi$ and $\varphi$ around the critical points.

### 3.7.1 Skew-Whiffed solutions

The simplest of the vacuum solutions[46, 54] with $\epsilon = -1$ are

$$\phi = 0, \quad \varphi = 0, \quad \partial_\rho\mathcal{A} = \pm 2, \tag{49}$$

with the radius squared of the $AdS$ metric being given by

$$R_{AdS}^2 = \frac{1}{4}. \tag{50}$$

It can be shown that these Skew-Whiffed $AdS_4 \times SE_7$ solutions generally do not preserve supersymmetry, except in the case where $SE_7$ is the seven-sphere and $N = 8$ supersymmetry

is preserved. Within a supergravity approximation, these vacua have well-defined dual CFT's, as they have been shown to be perturbatively stable [51].

In this background, we find that we have two massive scalars, with masses $m_\phi^2 = m_\varphi^2 = -8$ corresponding to $\Delta = 2$

### 3.7.2 Pope-Warner solutions

Another further set of vacuum solutions, known as the Pope-Warner solutions [55], have $\epsilon = -1$ and

$$\phi = 0, \quad \varphi = \pm \log(1 + \sqrt{2}), \quad \partial_\rho \mathcal{A} = \pm \frac{4}{\sqrt{3}}. \tag{51}$$

with the radius squared of the $AdS$ metric being given by

$$R_{AdS}^2 = \frac{3}{16}. \tag{52}$$

It can be shown that the Pope-Warner solutions do not preserve any supersymmetry for any choice of $SE_7$[56]. Again we end up with two massive scalars, this time with $m_\phi^2 = m_\varphi^2 = 32$ corresponding to a scaling parameter of $\Delta = \frac{3+\sqrt{33}}{2}$

### 3.7.3 Englert solutions

The last set of vacuum solutions we will consider are the Englert solutions [57], which have $\epsilon = -1$ and

$$\phi = \pm \log\left(\frac{1+\sqrt{5}}{2}\right), \quad \varphi = \pm \log\left(\frac{1+\sqrt{5}}{2}\right), \quad \partial_\rho \mathcal{A} = \pm \frac{5^{\frac{5}{4}}}{2\sqrt{3}}. \tag{53}$$

with the radius squared of the $AdS$ metric being given by

$$R_{AdS}^2 = \frac{12}{25\sqrt{5}}. \tag{54}$$

In general, this solution is unstable and can be shown to preserve no supersymmetry, both in the $S^7$ case and the more general $SE_7$ case [56]. The $D = 4$ theory in this background

gives two massive scalars with masses $m_\phi^2 = m_\varphi^2 = \frac{25\sqrt{5}}{2}$ corresponding to a scaling parameter of $\Delta = \frac{3+\sqrt{33}}{2}$.

# 4 New classical background solutions

We consider the fixed-point vacuum solutions to exist on the boundaries of the bulk geometry in the limit $z \to 0$. Starting from these analytic solutions, we can also construct numerical solutions that exist within the bulk and interpolate between the critical points. In this section, we further develop our analysis by finding some of these solutions and elaborating on how they may be constructed.

We begin this process of solution-finding in mathematica by solving equations of motion into which we have substituted a series expansion for each of the relevant scalars, in order to determine the unknown coefficients in said expansion, in terms of one or two 'free parameters'. As we shall state in more detail shortly, these expansions are near-boundary expansions that represent the values of the scalar fields in the limit we have defined as the boundary of space.

## 4.1 IR-Conformal solutions

The first family of solutions we will explore are those in which we place an IR and UV fixed point at opposite ends of the geometry, where the space becomes asymptotically $AdS$. Specifically, we will use the convention that our solutions approach the IR as $\rho \to -\infty$, and the UV as $\rho \to \infty$

The first step in computing such a one-parameter family of domain wall solutions which flow from a point in the IR is to expand the scalar fields $\phi(\rho)$ and $\varphi(\rho)$ in the limit of small $z^{d-\Lambda}$. To construct solutions which asymptote towards the Pope-Warner vacuum in the IR, as $\rho \to -\infty$, we consider the following near boundary expansion.

$$\phi = \phi_1 z^{3-\Delta} + \frac{8\sqrt{2}}{9-\sqrt{33}}\phi_1\varphi_1 z^{2(3-\Delta)} + \dots\,, \tag{55}$$

$$\varphi = \log(1+\sqrt{2}) + \varphi_1 z^{3-\Delta} + \frac{6\phi_1^2 + 9\varphi_1^2}{\sqrt{2}(9-\sqrt{33})} z^{2(3-\Delta)} + \dots\,, \tag{56}$$

$$\mathcal{A} = -\log(z) + \log(\frac{\sqrt{3}}{4}) + \frac{1}{16}(-3\phi_1^2 - 4\varphi_1^2) z^{2(3-\Delta)} + \dots\,, \tag{57}$$

Where $\Delta = \frac{3+\sqrt{33}}{2}$, and ,as per our rewriting of the metric, we have chosen $z = \frac{4}{\sqrt{3}} e^{-\frac{4}{\sqrt{3}}\rho}$.

In addition, we can demonstrate that there is a single domain wall solution which flows from the Englert vacuum in the IR to the Skew-whiffed vacuum in the UV, using the expansion

$$\phi = \log(\frac{1+\sqrt{5}}{2}) + \phi_1 z^{3-\Delta} + \frac{24}{\sqrt{5}(-9+\sqrt{33})}\phi_1^2 z^{2(3-\Delta)} + \dots \tag{58}$$

$$\varphi = \log(\frac{1+\sqrt{5}}{2}) + \phi_1 z^{3-\Delta} + \frac{24}{\sqrt{5}(-9+\sqrt{33})}\phi_1^2 z^{2(3-\Delta)} + \dots\,, \tag{59}$$

$$\mathcal{A} = -\log(z) + \log(\frac{12}{25\sqrt{5}}) - \frac{7}{16}\phi_1^2 z^{2(3-\Delta)} + \dots\,, \tag{60}$$

With $\Delta = \frac{3+\sqrt{33}}{2}$ and $z = \frac{12}{25\sqrt{5}} e^{-\frac{5^{\frac{5}{4}}}{2\sqrt{3}}\rho}$.

Recall that the scalar potential of the four-dimensional model has extrema for $(\phi, \varphi)$ at $(0,0)$, $(0, \pm\log(1+\sqrt{2})))$, and $(\pm\log(\frac{1+\sqrt{5}}{2}), \pm\log(\frac{1+\sqrt{5}}{2}))$, corresponding respectively to the Skew-Whiffed, Pope-Warner, and Englert $AdS$ vacua.

With this in mind, we present solutions that interpolate between the Pope-Warner vacuum in the IR, as $\rho \to -\infty$ and the Skew-Whiffed solutions in the UV, as $\rho \to \infty$.

In order to generate these solutions, we return to Mathematica and use the NDSolve function to construct numerical solutions for $-\infty < \rho < \infty$. Using NDsolve, solving the equations for the scalars $\phi$, $\varphi$, and $\mathcal{A}$ is treated as an initial value problem in which our initial values are provided by substituting our near-boundary solutions in the IR into the equations of motion. Different choices of the parameters $\phi_1$ and $\varphi_2$ in this substitution will produce different branches of solution.

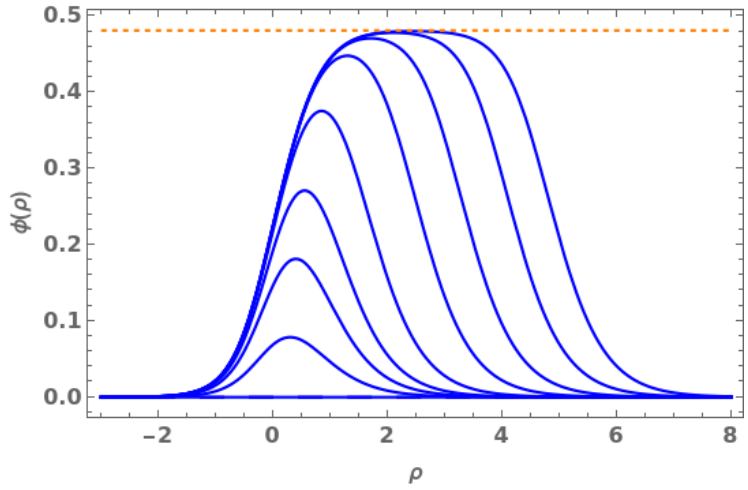


(a) $\phi(\rho)$

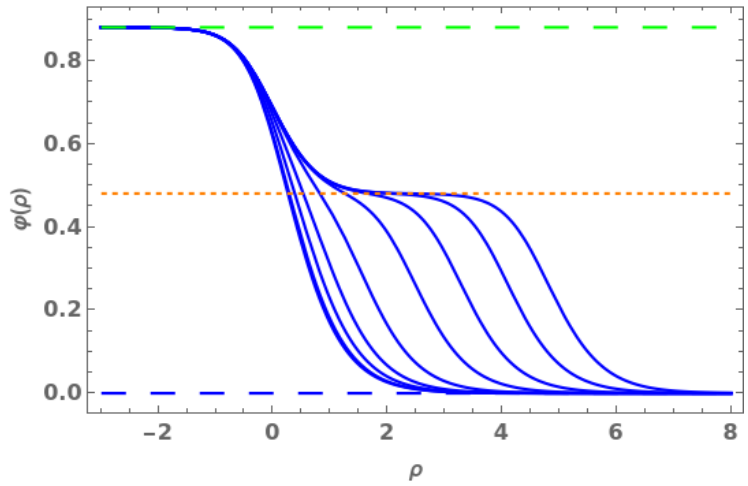


(b) $\varphi(\rho)$

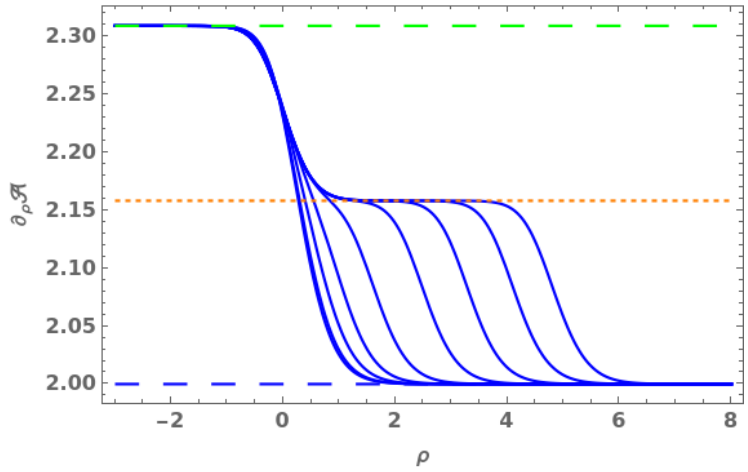


(c) $\partial_\rho \chi$

Figure 1: Solutions for functions $\phi(\rho)$, $\varphi(\rho)$, and $\partial_\rho A$ for the three-dimensional $\sigma$ model as a function of radial direction $\rho$. The blue curves show solutions for which $\varphi_I$ is kept constant and $\phi_I$ is varied. The orange dashed lines represent the Englert fixed point solutions for which $\phi = \varphi = \log(\frac{1+\sqrt{5}}{2})$.Only positive valued solutions are considered in these plots. We also include in each plot green, orange, and blue dashed lines that represent the value of the field at the Pope-Warner, Englert, and Skew-Whiffed fixed points respectively.

In interpreting these results, it is also worth reminding ourselves that in gauge theory terms, these interpolating solutions represent holographic RG flows between two CFT's, with our choice of the parameters $\phi_1$ and $\varphi_1$ dictating the scale at which the transition between these CFT's occurs, and how closely the solution comes to approaching the unstable Englert vacuum.

We can also construct an additional domain wall solution which flows from the Englert vacuum in the IR towards the Skew-Whiffed vacuum in the UV. We expect that there should also exist a single solution which interpolates between the Pope-Warner solution in the IR and the Englert solution in the UV. However, the Englert vacuum is unstable and as such it is extremely difficult to compute an exact numerical solution that asymptotes towards the critical point. However, we find that as we alter the ratio between the two IR parameters $\phi_1, \varphi_1$, the values of the scalar fields $\phi$ and $\varphi$ will flow from the PW vacuum towards the Englert fixed point, and for some interval of $\delta\rho$ will remain there before again flowing towards the SW vacuum in the UV. In particular, we note that as $\frac{\varphi_1}{\phi_1} \to 1 - \frac{\log(1+\sqrt{2})}{\log(\frac{1+\sqrt{5}}{2})}$, then $\delta\rho \to \infty$, allowing us to approximate solutions which interpolate to and from the Englert vacuum solutions. Nevertheless, given the aforementioned instability of the Englert vacua, the physical implications of these solutions are unclear.

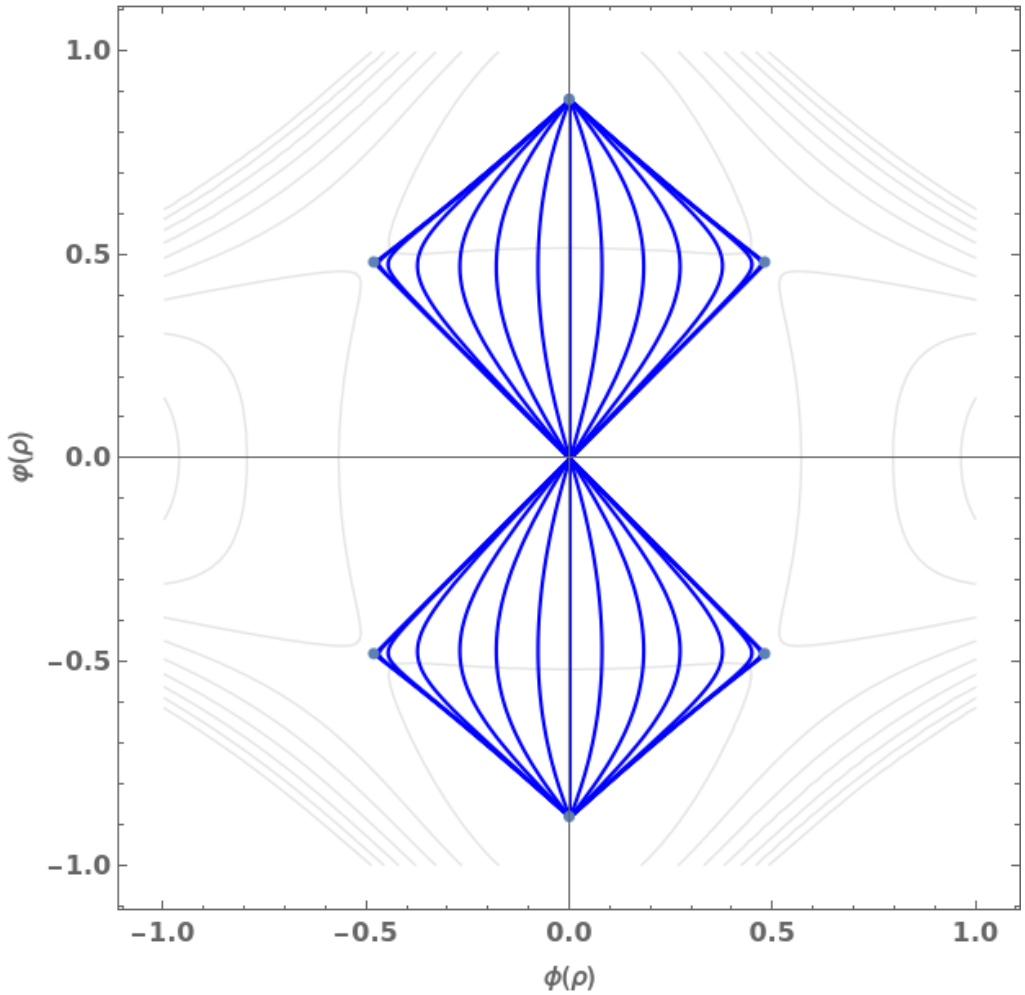


Figure 2: This plot displays the scalar potential of our model in the $\phi$-$\varphi$ plane, with the dots indicating extrema which correspond to the Skew-Whiffed, Pope-Warner, and Englert vacuum solutions. The solid lines represent domain wall solutions which interpolate between these fixed points. We take note of the very clear tendency of numerical solutions which start at the PW solution to approach the critical point corresponding to the Englert vacuum

## 4.2 Circle reduction

In order to consider the next class of classical solutions we must first adopt a new convention that represents an alternative compactification of 11-dimensional SUGRA. As before, the eleven-dimensional model is truncated to a four-dimensional supergravity, with the key distinction that one of these four dimensions is circular and periodic. The four-dimensional

metric is as follows:

$$ds_4^2 = e^{-2\chi(r)} ds_3^2 + e^{2\chi(r)} d\eta^2 \tag{61}$$

$$ds_3^2 = e^{2A(r)} dx_\mu dx^\mu + dr^2 \tag{62}$$

$$\partial_r = e^{-\chi} \partial_\rho \qquad\qquad 0 \leq \eta < 2\pi \tag{63}$$

where $\eta$ is the coordinate along a circle, $ds_3^2$ is the three-dimensional metric, $dx_\mu dx^\mu$ are the standard Euclidean dimensions, while $\chi$ and $A$ are scalar functions. In this analysis, we will require that the size of the circle is dependent on the radial coordinate $\rho$, such that the geometry closes smoothly for some finite value of $\rho$ and the circle shrinks to zero size.

We notice that in this background we recover the $AdS$ metric at the end of space in the limit $A = 2\chi = 2\mathcal{A}$, as the circular dimension diverges to infinite size.

Now, in four dimensions, the action of pure gravity can be written as

$$\int d^4x \sqrt{-g_4} \left[ \frac{R_4}{4} - V \right]. \tag{64}$$

In addition, we may also write a three-dimensional action in which the only scalar coupled to gravity is $\chi$, where,

$$\mathcal{S}_3 = \int d^3x \sqrt{-g_3} \left[ \frac{R_3}{4} - \frac{1}{2} G_{\chi\chi} g^{MN} \partial_M \chi \partial_N \chi - V_3 \right]. \tag{65}$$

Using the ansatz provided, then the three and four-dimensional Ricci scalars are

$$R_3 = e^{-2\chi(\rho)} \left( (-6\partial_\rho A)^2 - 4\partial_\rho^2 A + 4\partial_\rho A \partial_\rho \chi \right) \qquad - g_3 = e^{4A(\rho)+2\chi(\rho)}, \tag{66}$$

$$R_4 = -4\partial_\rho^2 A - 4(\partial_\rho \chi)^2 + 8\partial_\rho A \partial_\rho \chi - 6(\partial_\rho A)^2 + 2\partial_\rho^2 \chi \qquad - g_4 = e^{4A(\rho)-2\chi(\rho)}, \tag{67}$$

and as such, with $G_{\chi\chi} = 1$, we may rewrite the three and four-dimensional action as

$$\mathcal{S}_4 = \int e^{2A(\rho)-\chi(\rho)} \left[ \partial_\rho A \partial_\rho \chi - \partial_\rho^2 A - \frac{3}{2}(\partial_\rho A)^2 - \frac{1}{2}(\partial_\rho \chi)^2 - V \right] + \partial_\rho \left( \frac{1}{2} e^{2A(\rho)-\chi(\rho)} \partial_\rho \chi \right) d^4x, \tag{68}$$

$$\mathcal{S}_3 = \int e^{2A(\rho)-\chi(\rho)} \left[ \partial_\rho A \partial_\rho \chi - \partial_\rho^2 A - \frac{3}{2}(\partial_\rho A)^2 - \frac{1}{2}(\partial_\rho \chi)^2 - e^{2\chi(\rho)} V_3 \right] d^3x. \tag{69}$$

If we further identify

$$\partial\mathcal{S} = \int \partial_M \left( \frac{1}{2} \sqrt{-g_3} g^{MN} \partial_N \chi \right) d^3x \tag{70}$$

$$= \int \partial_\rho \left( \frac{1}{2} e^{2A(\rho)-\chi(\rho)} \partial_\rho \chi \right) d^3x \tag{71}$$

and

$$V_3 = e^{-2\chi(\rho)} V \tag{72}$$

then it becomes clear that one may rewrite the four-dimensional action $\mathcal{S}_4$ in terms of the four-dimensional action $\mathcal{S}_3$, and the derivative $\partial\mathcal{S}$, such that

$$\mathcal{S}_4 = 2\pi \left( \mathcal{S}_3 + \partial\mathcal{S} \right) \tag{73}$$

More importantly however, is that because $\partial\mathcal{S}$ is a total derivative, then the four-dimensional equations of motion admit solutions which are also solutions to the equations of motion derived in the three-dimensional background. In other words, the addition of a total derivative to the Lagrangian leaves the action invariant, and as such, represents a physical symmetry of the system.

### 4.2.1 Equations of motion

Starting with the three-dimensional action with scalar $\chi$ coupled to gravity given in equation (65), we add kinetic terms for scalars $\phi$ and $\varphi$. Thus, if we additionally specify

$$G_{ab} = \begin{pmatrix} \frac{3}{4} & 0 & 0 \\ 0 & 1 & 0 \\ 0 & 0 & 1 \end{pmatrix}, \tag{74}$$

$$V = \frac{1}{2}\cosh(3\phi)\sinh^2(2\varphi) - 6\cosh(\phi)\cosh^2(\varphi), \tag{75}$$

then the three-dimensional equations of motion for the action of scalars $\{\phi, \varphi, \chi\}$ coupled to gravity are

$$\partial_\rho^2\phi + \partial_\rho\phi(2\partial_\rho A - \partial_\rho\chi) - \frac{4}{3}\frac{\partial V}{\partial\phi} = 0, \tag{76}$$

$$\partial_\rho^2\varphi + \partial_\rho\varphi(2\partial_\rho A - \partial_\rho\chi) - \frac{\partial V}{\partial\varphi} = 0, \tag{77}$$

$$\partial_\rho^2\chi + \partial_\rho\chi(2\partial_\rho A - \partial_\rho\chi) + 2V = 0, \tag{78}$$

and the Einstein equations are

$$\partial_\rho^2 A + \partial_\rho A(2\partial_\rho A - \partial_\rho\chi) + 4V = 0, \tag{79}$$

$$-\frac{3}{2}(\partial_\rho\phi)^2 - 2(\partial_\rho\varphi)^2 - 2(\partial_\rho\chi)^2 + 2(\partial_\rho A)^2 + 4V = 0. \tag{80}$$

At this point, we will take note of a useful conserved quantity whose use will later become clear, obtained by subtracting equation (79) from equation (78) multiplied by 2. Doing so gives us.

$$2\partial_\rho^2\chi - \partial_\rho^2 A + 5\partial_\rho\chi\partial_\rho A - 2\partial_\rho A - 2\partial_\rho\chi = 0, \tag{81}$$

which after multiplying by a factor of $e^{2A-\chi}$ and some careful integration by parts, gives us

$$\partial_\rho(e^{2A(\rho)-\chi(\rho)}(2\partial_\rho\chi - \partial_\rho A)) = 0 \tag{82}$$

### 4.2.2 Confining Solutions

We turn our attention to a class solutions of the equations of motion which have constant $\phi(\rho) = \phi_0$, and $\varphi(\rho) = \varphi_0$, where $\phi_0$, $\varphi_0$ are equivalent to the fixed point $AdS$ solutions presented in (49), (51), and (53), and confine at the end of space $\rho = 0$. these $AdS$-Soliton solutions take the form

$$\phi(\rho) = \phi_0, \tag{83}$$

$$\varphi(\rho) = \varphi_0, \tag{84}$$

$$\chi(\rho) = \chi_I + \log\left[\sinh\left(\frac{3}{2}\chi_0\rho\right)\right] - \frac{1}{3}\log\left[\cosh\left(\frac{3}{2}\chi_0\rho\right)\right], \tag{85}$$

$$A(\rho) = A_I + \log\left[\sinh\left(\frac{3}{2}\chi_0\rho\right)\right] + \frac{1}{3}\log\left[\cosh\left(\frac{3}{2}\chi_0\rho\right)\right], \tag{86}$$

where $\chi_0$ is equivalent to one of the three fixed point solutions of $\partial_\rho\mathcal{A}$ detailed in section 3.7. The integration constants $\chi_I$ and $A_I$ are fixed by the requirement that the four-dimensional metric (61) remains regular at the end of space $\rho_0 = 0$ and we avoid a conical singularity in the geometry. Expanding for small $\rho$, the metric takes the form

$$ds_4^2 = d\rho^2 + e^{2(A_I-\chi_I)}dx_\mu dx^\mu + \left(\frac{3\chi_0}{2}e^{\chi_I}\right)^2\rho^2 d\eta^2. \tag{87}$$

As $\eta$ is a periodic coordinate with period $2\pi$, then it follows that $\chi_I = -\log(\frac{3\chi_0}{2})$ if we wish to avoid producing an angular deficit. As for $A_I$, given that the constant can be absorbed via a rescaling of the Euclidean/Minkowski coordinates, we will, by convention, set $A_I = \chi_I$ [23]. Therefore, for each of the three possible confining solutions we have the corresponding values for the integration constant $\chi_I$:

$$\chi_I = -\log(3), \tag{88}$$

$$\chi_I = -\log(2\sqrt{3}), \tag{89}$$

$$\chi_I = -\log\left(\frac{5^{\frac{5}{4}}\sqrt{3}}{4}\right), \tag{90}$$

We note again that for large values $\rho \gg 1$ we find that $A \simeq 2\chi$ and that, in the UV, the $AdS$ geometry is recovered.

### 4.2.3 Multi-scale confining solutions

Just as we were able to construct interpolating solutions between the fixed point $AdS$ vacua in the previous chapter, in this background we may also construct general solutions which flow from a fixed point in the UV towards another in the IR. In the context of the dual CFT's, these multi-scale solutions again represent RG flows between an IR CFT and a UV CFT, where each flow is defined by a characteristic energy scale at which the transition between the two theories takes place. However, our choice of paramaterisation also defines an additional confinement scale at which the scalar mass spectrum is discretized into bound states. When working within the gravity theory, we define this scale at which the circular coordinate $\eta$ becomes zero and the circular dimension shrinks to zero size.

Our first step in generating these multi-scale solutions is to consider the IR expansion for small $\rho$, where the space closes off smoothly at $\rho = 0$, of the form

$$\begin{aligned}\phi(\rho) &= \phi_I + \frac{1}{2}\rho^2\left(\sinh(3\phi_I)\sinh^2(2\varphi_I) - 4\sinh(\phi_I)\cosh^2(\varphi_I)\right)\\ &\quad +\frac{1}{8}\rho^4\left(\sinh^2(2\varphi_I)(\sinh(6\phi_I)\cosh(4\varphi_I) - 4\sinh(4\phi_I)(2\cosh(2\varphi_I)+1))\right.\\ &\quad \left.-2\sinh(2\phi_I)\cosh^2(\varphi_I)(\cosh(4\varphi_I) - 9\cosh(2\varphi_I))\right) + \mathcal{O}(\rho^6), \qquad (91)\end{aligned}$$

$$\begin{aligned}\varphi(\rho) &= \varphi_I + \frac{1}{4}\rho^2(\cosh(3\phi_I)\sinh(4\varphi_I) - 6\cosh(\phi_I)\sinh(2\varphi_I))\\ &\quad +\frac{1}{128}\rho^4\left(\sinh(4\varphi_I)(84\cosh(2\phi_I) - 24\cosh(4\phi_I) - 4\cosh(6\phi_I) + 62)\right.\\ &\quad -18\sinh(6\varphi_I)(\cosh(2\phi_I) + 2\cosh(4\phi_I)) + \sinh(8\varphi_I)(4\cosh(6\phi_I)+1)\\ &\quad \left.+6\sinh(2\varphi_I)(17\cosh(2\phi_I) + 2\cosh(4\phi_I) + 8)\right) + \mathcal{O}(\rho^6), \qquad (92)\end{aligned}$$

$$\begin{aligned}\chi(\rho) &= \chi_I + \log(\rho) + \frac{1}{160}\rho^4 \left(8\cosh^2(\varphi_I)(\cosh(2\varphi_I)(2 - 9\cosh(2\phi_I)) + 21\cosh(2\phi_I) + 22)\right. \\ &\quad \left. - \sinh^2(2\varphi_I)(\cosh(6\phi_I)(3\cosh(4\varphi_I) + 1) - 24\cosh(4\phi_I)\cosh(2\varphi_I))\right) + \mathcal{O}(\rho^6), \quad (93)\end{aligned}$$

$$\begin{aligned}A(\rho) &= \chi_I + \log(\rho) + \frac{1}{4}\rho^2 \left(12\cosh(\phi_I)\cosh^2(\varphi_I) - \cosh(3\phi_I)\sinh^2(2\varphi_I)\right) \\ &\quad + \frac{1}{1280}\rho^4 \left(96\cosh(2\phi_I)\cosh^2(\varphi_I)(-51\cosh(2\varphi_I) + 5\cosh(4\varphi_I) + 14)\right. \\ &\quad + 8\sinh^2(2\varphi_I)(12\cosh(4\phi_I)(12\cosh(2\varphi_I) + 5) - \cosh(6\phi_I)(13\cosh(4\varphi_I) + 1)) \\ &\quad \left. - 192\cosh(2\varphi_I) - 588\cosh(4\varphi_I) - 5\cosh(8\varphi_I) + 401\right) + \mathcal{O}(\rho^6). \quad (94)\end{aligned}$$

Where we have retained the integration constant $\chi_I$ from the simple confining solutions, and introduced the integration constants $\phi_I$ and $\varphi_I$. The ratio between these two parameters will determine the scale at which a given flow from the UV to the IR theory take place, while the individual choices of their values will determine the scale at which the operators dual to the scalar fields $\phi$ and $\varphi$ confine. Below, we present a series of numerically evaluated multi-scale confining solutions which interpolate between the Pope-Warner and Skew-whiffed fixed point solutions. In order to demonstrate how the dual theory confines, while also demonstrating how certain classes of solution approach the Englert fixed point, we first present flows generated by varying only $\varphi_I$, and before varying both parameters together. In the final case, our choice of starting values is taken from points lying along a single class of interpolating solutions, such that we vary both $\phi_I$ and $\varphi_I$ to obtain a set of results.

They key observation to be made here is that solutions defined by $\varphi_I < \log(1+\sqrt{2}), \phi > 0$ fail to reach the IR fixed point before the space smoothly closes off at $\rho_0 = 0$. In the language of Gauge theory, this corresponds to the scale of confinement being larger than the scale at which we should have observed RG flows from the UV theory. As a result, the theory confines well before the physics of the system can be probed by the IR CFT. In the limit of $\varphi_I \to 0$, in particular, the theory confines immediately and the solution remains fixed at its UV solution. Conversely, in the opposite limit as $\varphi_I \to \log(1+\sqrt{2})$, it can be seen that the scale of confinement is smaller than the scale at which RG flows take place, and there is

therefore some characteristic energy scale at which our system may be described by the IR CFT.

We also continue to observe the behaviour demonstrated by previous interpolating flows where our choice of parameterisation affects the tendency of the solution to approach the unstable Englert vacuuum before arriving at the Skew-Whiffed vacua in the UV. For the confining solutions, we note that this occurs as $\varphi_I \to \left(1 - \frac{\log(1+\sqrt{2})}{\log(1+\sqrt{2})}\right)\phi_I + \log(1+\sqrt{2})$, for some non-zero starting value of parameter $\phi_I$. An interesting behaviour is observed in figure 4, however. Despite the starting points used to evaluate each solution being taken from successive points on the same 'primary' interpolating solution, they each can be seen to diverge from this primary solution in terms of how closely they approach the Englert fixed point. Due to the shape of the potential $V(\phi, \varphi)$, this behaviour appears to be related to the proximity of $\phi_I$ and $\varphi_I$ to some point approximately midway between the Pope-Warner solution and Englert solution in the $\phi - \varphi$ parameter space. The closer the proximity, the closer the evaluated numerical solution tends towards the Englert point.

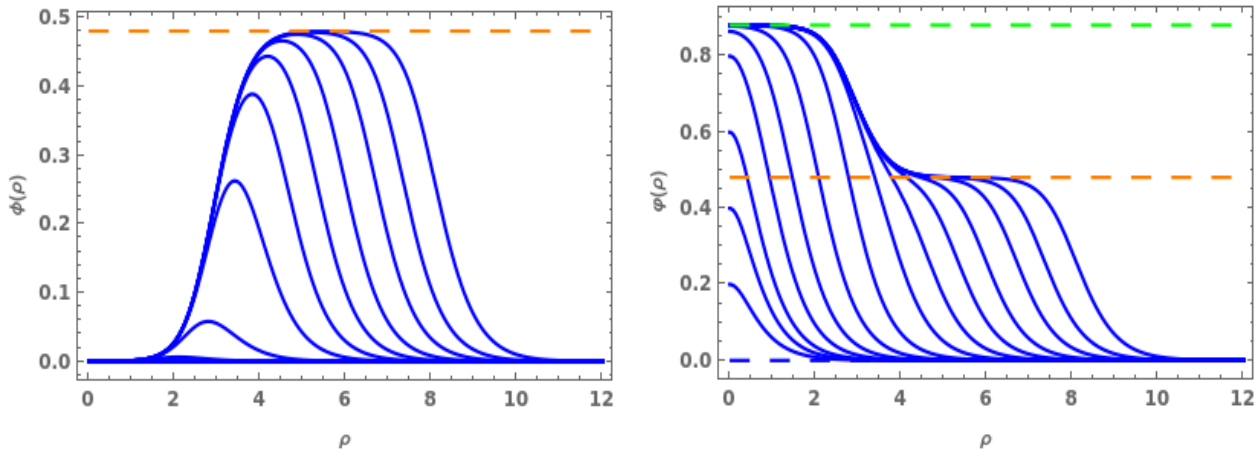


(a) $\phi(\rho)$




(b) $\varphi(\rho)$

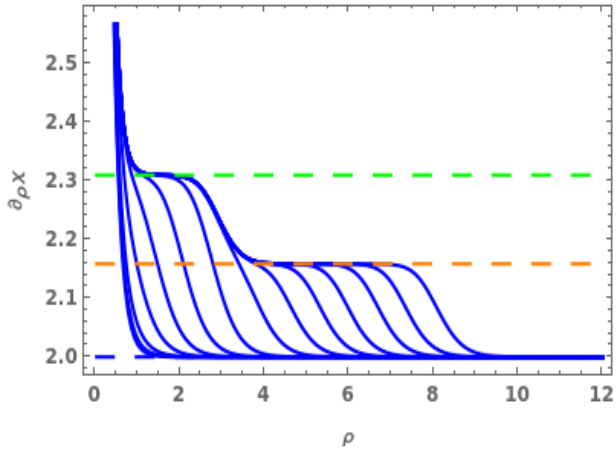


(c) $\partial_\rho \chi$

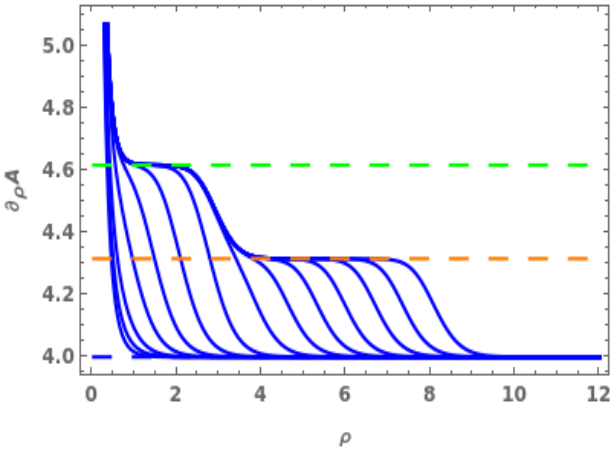


(d) $\partial_\rho A$

Figure 3: Solutions for functions $\phi(\rho)$, $\varphi(\rho)$, $\partial_\rho \chi$, and $\partial_\rho A$ for the three-dimensional $\sigma$ model as a function of radial direction $\rho$. The blue curves show solutions for which $\varphi_I$ is kept constant and $\phi_I$ is varied. The orange dashed lines represent the Englert fixed point solutions for which $\phi = \varphi = \log(\frac{1+\sqrt{5}}{2})$, while the green dashed solutions are dual to conformal Pope-Warner vacuum ($\varphi = \log(1+\sqrt{2})$) in the IR. We have also included a blue dashed line representative of the Skew-Whiffed fixed point whose dual immediately confines. Only positive valued solutions are considered in these plots. As we increase the value of our choice of $\phi_I$, the RG flows dual to these supergravity solutions become nearly scale invariant between the IR and the UV in the vicinity of the Englert critical point.

fire

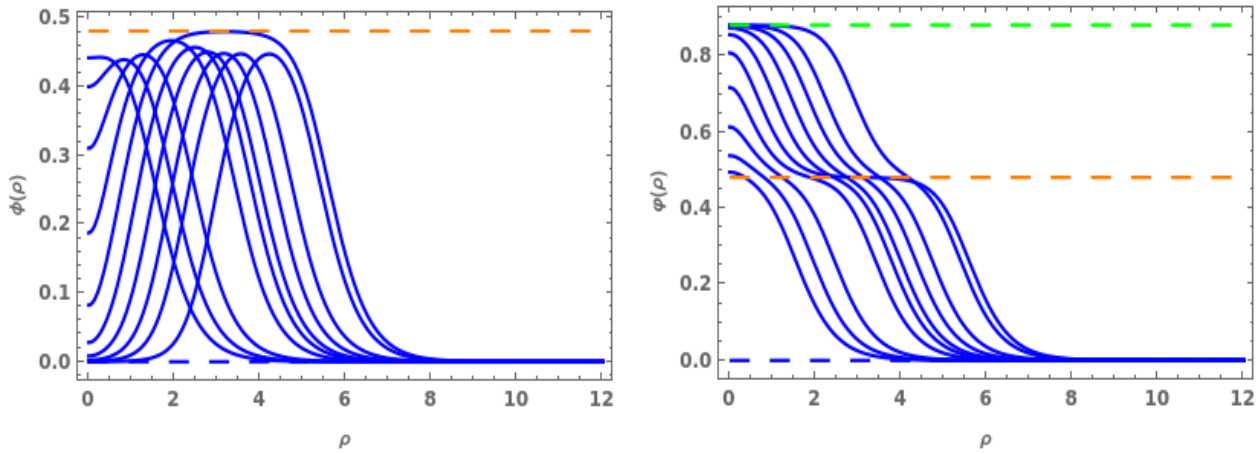


(a) $\phi(\rho)$




(b) $\varphi(\rho)$

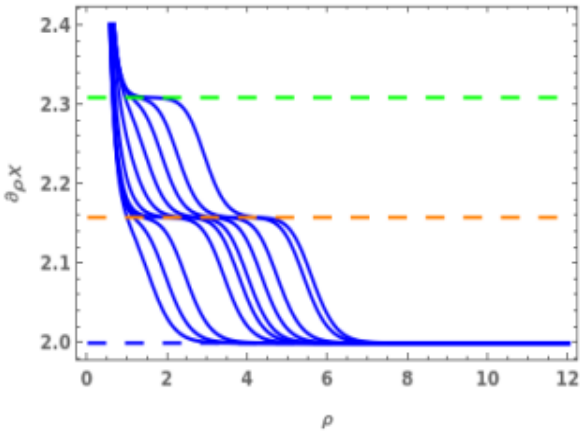


(c) $\partial_\rho \chi$

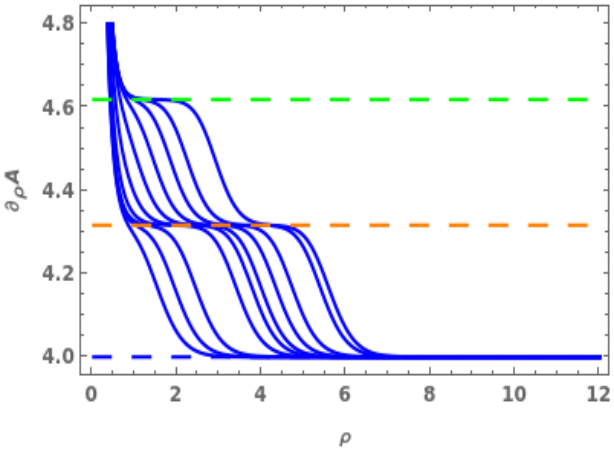


(d) $\partial_\rho A$

Figure 4: Solutions for functions $\phi(\rho)$, $\varphi(\rho)$, and $\partial_\rho A$ for the three-dimensional $\sigma$ model as a function of radial direction $\rho$. The blue curves show solutions for which both $\varphi_I$ and $\phi_I$ is varied. The orange dashed lines represent the Englert fixed point solutions for which $\phi = \varphi = \log(\frac{1+\sqrt{5}}{2})$.Only positive valued solutions are considered in these plots

# 5 Free energy

## 5.1 Ultraviolet Reparamaterisation

Before we discuss in detail the relationship between the free energy and the UV parameters for both of the distinct types of solutions, we must first detail the procedure of scale setting and reparameterisation which will be required to properly interpret our results. Our discussion necessarily starts with the expansions for both scalars in the vicinity of the UV fixed point, for both the confining and conformal solutions. As both classes of solution are asymptotically

$AdS$ in the limit of $\rho \to \infty$, they permit the same near boundary expansion in this limit:

$$\phi(z) = \phi_1 z + \phi_2 z^2 + \frac{1}{48} z^3 \left(132\phi_1\varphi_1^2 + 19\phi_1^3\right) + \frac{1}{24} z^4 \left(48\phi_1\varphi_1\varphi_2 + 28\phi_2\varphi_1^2 + 17\phi_2\phi_1^2\right) + \quad (95)$$
$$\frac{1}{3840} z^5 \left(17160\phi_1^3\varphi_1^2 + 14160\phi_1\varphi_1^4 + 2240\phi_1\varphi_2^2 + 5120\phi_2\varphi_1\varphi_2 + 723\phi_1^5 + 2320\phi_2^2\phi_1\right) +$$
$$\frac{1}{3840} z^6 \left(15744\phi_1^3\varphi_1\varphi_2 + 28472\phi_2\phi_1^2\varphi_1^2 + 26880\phi_1\varphi_1^3\varphi_2 + 7184\phi_2\varphi_1^4 + 1920\phi_2\varphi_2^2 + 2405\phi_2\phi_1^4 + 800\phi_2^3\right),$$

$$\varphi(z) = \varphi_1 z + \varphi_2 z^2 + \frac{1}{48} z^3 \left(99\phi_1^2\varphi_1 + 52\varphi_1^3\right) + \frac{1}{8} z^4 \left(7\phi_1^2\varphi_2 + 12\phi_2\phi_1\varphi_1 + 12\varphi_1^2\varphi_2\right) + \quad (96)$$
$$\frac{1}{3840} z^5 \left(21240\phi_1^2\varphi_1^3 + 6435\phi_1^4\varphi_1 + 1680\phi_2^2\varphi_1 + 3840\phi_1\phi_2\varphi_2 + 4368\varphi_1^5 + 4160\varphi_2^2\varphi_1\right) +$$
$$\frac{1}{3840} z^6 \left(2853\phi_1^4\varphi_2 + 12768\phi_2\phi_1^3\varphi_1 + 33816\phi_1^2\varphi_1^2\varphi_2 + 19200\phi_2\phi_1\varphi_1^3 + 1440\phi_2^2\varphi_2 + 1280\varphi_2^3 + 12048\varphi_1^4\varphi_2\right),$$

$$A(z) = A_0 - 2\log(z) + \frac{1}{8} z^2 \left(-3\phi_1^2 - 4\varphi_1^2\right) + \frac{2}{9} z^3 \left(3\chi_3 - 3\phi_1\phi_2 - 4\varphi_1\varphi_2\right) + \quad (97)$$
$$\frac{1}{256} z^4 \left(-792\phi_1^2\varphi_1^2 - 57\phi_1^4 - 96\phi_2^2 - 208\varphi_1^4 - 128\varphi_2^2\right) +$$
$$\frac{1}{40} z^5 \left(9\chi_3\phi_1^2 - 140\phi_1^2\varphi_1\varphi_2 - 140\phi_2\phi_1\varphi_1^2 - 25\phi_2\phi_1^3 + 12\chi_3\varphi_1^2 - 80\varphi_1^3\varphi_2\right) +$$
$$\frac{1}{55296} z^6 \left(-36864\chi_3^2 + 18432\chi_3\phi_2\phi_1 - 317196\phi_1^4\varphi_1^2 - 535248\phi_1^2\varphi_1^4 - 56448\phi_1^2\varphi_2^2 -\right.$$
$$\left. 208896\phi_2\phi_1\varphi_1\varphi_2 - 56448\phi_2^2\varphi_1^2 - 7587\phi_1^6 - 40032\phi_2^2\phi_1^2 + 24576\chi_3\varphi_1\varphi_2 - 67392\varphi_1^6 - 107008\varphi_1^2\varphi_2^2\right),$$

$$\chi(z) = \chi_0 - \log(z) + \frac{1}{16} z^2 \left(-3\phi_1^2 - 4\varphi_1^2\right) + \frac{1}{9} z^3 \left(12\chi_3 - 3\phi_1\phi_2 - 4\varphi_1\varphi_2\right) + \quad (98)$$
$$\frac{1}{512} z^4 \left(-792\phi_1^2\varphi_1^2 - 57\phi_1^4 - 96\phi_2^2 - 208\varphi_1^4 - 128\varphi_2^2\right) +$$
$$\frac{1}{80} z^5 \left(36\chi_3\phi_1^2 - 140\phi_1^2\varphi_1\varphi_2 - 140\phi_2\phi_1\varphi_1^2 - 25\phi_2\phi_1^3 + 48\chi_3\varphi_1^2 - 80\varphi_1^3\varphi_2\right) +$$
$$\frac{1}{110592} z^6 \left(-36864\chi_3^2 + 73728\chi_3\phi_2\phi_1 - 317196\phi_1^4\varphi_1^2 - 535248\phi_1^2\varphi_1^4 - 56448\phi_1^2\varphi_2^2 -\right.$$
$$\left. 208896\phi_2\phi_1\varphi_1\varphi_2 - 56448\phi_2^2\varphi_1^2 - 7587\phi_1^6 - 40032\phi_2^2\phi_1^2 + 98304\chi_3\varphi_1\varphi_2 - 67392\varphi_1^6 - 107008\varphi_1^2\varphi_2^2\right).$$

For us to appropriately compare both classes of solution, we make the choice to set the integration constants $A_0$ and $\chi_0$ equal to zero for all possible solutions. We find that setting $A_0$ is trivial due to the fact that the equations of motion are invariant under some shift in $A(\rho)$, as the free parameters in its expansion are set by $\phi$, $\varphi$, and $\chi$. Assigning a value to $\chi_0$ on the other hand, requires us to perform a rescaling of the radial coordinate $z$, which translates to a simple coordinate shift in the radial coordinate $\rho$.

In order to do this, for each numerical solution, we match the numerical value of the solution to some 'boundary' value $\rho = \rho_{UV}$, with its corresponding UV expansion in order to determine the value of $\chi_0$. We then reevaluate the numerical solutions using the coordinate shift $z \to ze^{\frac{\chi_0}{2}}$. This has the desired effect of setting the integration constant $\chi_0$ to zero in the reevaluated solutions.

For a proper analysis of the free energy, we require an additional scale setting procedure that will facilitate comparison between different classes of solutions. As previously discussed, for the confining solutions there is a parameter $\chi_0$ present in the IR expansions which must be fixed in order to avoid a conical singularity in the geometry of the space at small $\rho$. However, for the IR conformal/$AdS$ there is no such requirement set by the geometry, and, as such, we can see that the dimensionality of the free parameter space of the conformal solutions is greater than that of the confining solutions.

From the metric in (61), one can treat a rescaling of the coordinates $x^\mu \to \lambda x^\mu$ and $\eta^\mu \to \lambda\eta^\mu$ as exactly equivalent to an additive shift in the values of $A$ and $\chi$ as $A \to A + 2\log(\lambda)$ and $\chi \to \chi + \log(\lambda)$. However, in order to ensure $\chi_0$ and $A_0$ remain equal to zero, we must add to this a shift of $\rho \to \rho - \frac{1}{2}\log(\lambda)$. We see that under this transformation, $z \to \lambda z$, and as such our scalars transform as $\phi_n \to \lambda^n \phi_n$, where $\phi_n$ is a generic scalar field

Following the prescription set in [58], we can define a quantity $\Lambda$ which we will use to set an invariant characteristic energy scale. Specifically we define the quantity $\Lambda^{-1}$ as the time taken by a massless particle to reach the end of space from the UV boundary,

$$\Lambda^{-1} = \int_{r_0}^{\infty} d\tilde{r} e^{-A(\tilde{r})} = \int_{\rho_0}^{\infty} d\tilde{\rho} e^{\chi(\tilde{\rho}) - A(\tilde{\rho})}. \tag{99}$$

Under the above mentioned coordinate-shift, we have that $\Lambda \to \lambda\Lambda$, and therefore, we immediately find that we can define $\hat{\phi_n} \equiv \phi_n \Lambda^{-n}$ as a dimensionless quantity. As such, any analysis going forward will be described in units of $\Lambda$

## 5.2 General formalism

In order to begin our analysis of the free energy F and the free energy density $\mathcal{F}$ we must derive the free energy for our solutions from the action of the fields $\phi$ and $\varphi$ coupled to gravity in $D = 4$ dimensions. The free energy is related to the truncated action by

$$F \equiv -\lim_{\rho_1 \to \rho_0} \lim_{\rho_2 \to \infty} \mathcal{S} = \int d^2x d\eta \; \mathcal{F}. \tag{100}$$

We note that here we have included a regulator at both ends of the space, ensuring that for our calculations, the physical space is bounded by $\rho_1 < \rho < \rho_2$. In the UV, we will eventually recover the results of the physical field theory by taking $\rho_2 \to \infty$. In the IR, we understand that we must take $\rho_1 \to \rho_0$, where $\rho_0$ is the physical end of the geometry in the case of the confining solutions, or the opposite boundary of the space at infinity in the case of the IR-conformal solutions.

We start by defining the bulk four-dimensional action $\mathcal{S}_{bulk}$ for scalars $\phi$ and $\varphi$ coupled to gravity, where we write out the full scalar curvature and kinetic terms.

$$\mathcal{S}_{bulk} = \int_{\rho_1}^{\rho_2} d^2x d\rho d\eta \; \sqrt{-g_4} \left[ \frac{R_4}{4} - \frac{1}{2} G_{ab} g^{MN} \partial_M \phi_a \partial_N \phi_b - V \right], \tag{101}$$

$$= \int_{\rho_1}^{\rho_2} d^2x d\rho d\eta \; e^{2A(\rho) - \chi(\rho)} \left[ \frac{R_4}{4} - \frac{3}{8} (\partial_\rho \phi)^2 - \frac{1}{2} (\partial_\rho \varphi)^2 - V \right]. \tag{102}$$

Where the four-dimensional scalar curvature $R_4$ is given in (67). Substituting this into our action, and using equations of motion (76) and (77), we can remove the potential and kinetic terms from the bulk Lagrangian such that we have

$$\mathcal{S}_{bulk} = \int_{\rho_1}^{\rho_2} d^2x d\rho d\eta \; e^{2A(\rho)-\chi(\rho)} \left[\frac{3}{2}\partial_\rho A \partial_\rho \chi - \frac{1}{2}\partial_\rho^2 A - (\partial_\rho A)^2 + \frac{1}{2}\partial_\rho^2 \chi - \frac{1}{2}(\partial_\rho \chi)^2\right] \tag{103}$$

$$= -\frac{1}{2}\int_{\rho_1}^{\rho_2} d^2x d\rho d\eta \; \partial_\rho \left(e^{2A(\rho)-\chi(\rho)}\partial_\rho A\right) + \frac{1}{2}\int_{\rho_1}^{\rho_2} d^2x d\rho d\eta \; \partial_\rho \left(e^{2A(\rho)-\chi(\rho)}\partial_\rho \chi\right) \tag{104}$$

$$= -\frac{1}{4}\int_{\rho_1}^{\rho_2} d^2x d\rho d\eta \; \partial_\rho \left(e^{2A(\rho)-\chi(\rho)}\partial_\rho A\right), \tag{105}$$

Where in the final step we have made use of the conserved quantity $\partial_\rho(e^{2A(\rho)-\chi(\rho)}(2\partial_\rho\chi - \partial_\rho A)) = 0$, In order to write the action in terms of a total derivative.

Thus we have

$$\mathcal{S}_{bulk,i} = (-1)^{i+1}\frac{1}{4}\int d^2x \left(e^{2A(\rho)-\chi(\rho)}\partial_\rho A\right)\Big|_{\rho_i}, \tag{106}$$

where $i$ takes the value 1 or 2 depending on which end of the space we are evaluating the action. As we are working with a space in which there are boundaries, In general we must also include the contributions from the boundary localised potential and Gibbons-Hawkins-York terms [28, 29], evaluated on-shell, such that the total action $\mathcal{S}$ is given by

$$\mathcal{S} = \sum_{i=1,2} \left(\mathcal{S}_{bulk,i} + \mathcal{S}_{GHY,i} + \mathcal{S}_{pot,i}\right), \tag{107}$$

where

$$\mathcal{S}_{GHY,i} = (-1)^i \int d^2x d\eta \; \sqrt{-\hat{g}}\left(\frac{K}{2}\right)\Big|_{\rho=\rho_i}, \tag{108}$$

$$\mathcal{S}_{pot,i} = (-1)^i \int d^2x d\eta \; \sqrt{-\hat{g}}\left(\lambda_i\right)\Big|_{\rho=\rho_i}, \tag{109}$$

and the extrinsic curvature K is given by

$$K \equiv g^{MN}K_{MN} = g^{MN}\nabla_M n_N = -g^{MN}\Gamma^5_{MN} = 2\partial_\rho A - \partial_\rho \chi. \tag{110}$$

Using each of the above definitions leaves us with the general result

$$\mathcal{F} = \lim_{\rho_1 \to \rho_0} e^{2A(\rho)-\chi(\rho)} \left( \frac{3}{4}\partial_\rho A - \frac{1}{2}\partial_\rho \chi + \lambda_1 \right) \Big|_{\rho=\rho_1} - \lim_{\rho_2 \to \infty} e^{2A(\rho)-\chi(\rho)} \left( \frac{3}{4}\partial_\rho A - \frac{1}{2}\partial_\rho \chi + \lambda_2 \right) \Big|_{\rho=\rho_2} . \tag{111}$$

.

Now, our choice of $\lambda_2$ is based upon the requirement that all divergences cancel. We adopt the prescription that $\lambda_2 = \mathcal{W}_2$, where $\mathcal{W}_2$ is the superpotential $\mathcal{W}_2 = -2 - \frac{3}{4}\phi^2 - \varphi^2$. Making use of the UV expansions and the relation $\partial_\rho A = -2z\partial_z A$, we find,

$$\mathcal{S}_{GHY,2} = \int d^2x d\eta \, \frac{e^{2A_0-\chi_0}}{z^3} \left( 3 + \frac{9}{8}\phi_1^2 z^2 + \frac{3}{2}\varphi_1^2 z^2 + 3\phi_1\phi_2 z^3 + 4\varphi_1\varphi_2 z^3 \right) \Big|_{\rho_2} , \tag{112}$$

$$\mathcal{S}_{pot,2} = \int d^2x d\eta \, \frac{e^{2A_0-\chi_0}}{z^3} \left( -2 - \frac{3}{4}\phi_1^2 z^2 - \varphi_1^2 z^2 - \frac{3}{2}\phi_1\phi_2 z^3 - 2\varphi_1\varphi_2 z^3 \right) \Big|_{\rho_2} , \tag{113}$$

$$\mathcal{S}_{bulk,2} = \int d^2x d\eta \, \frac{e^{2A_0-\chi_0}}{z^3} \left( -1 - \frac{3}{8}\phi_1^2 z^2 - \frac{1}{2}\varphi_1^2 z^2 - \frac{3}{4}\phi_1\phi_2 z^3 - \varphi_1\varphi_2 z^3 - \frac{3}{4}\chi_3 z^3 \right) \Big|_{\rho_2} \tag{114}$$

where one can see that the quadratic divergences exactly cancel.

A choice of $\lambda_1 = -\frac{1}{2}\partial_\rho A$, allows us to write the full action at $\rho_1$

$$\mathcal{S}_{bulk,1} + \mathcal{S}_{GHY,1} + \mathcal{S}_{pot,1} = \frac{1}{4} \int d^2x d\eta \, \left( e^{2A(\rho)-\chi(\rho)} \left( 2\partial_\rho \chi - \partial_\rho A \right) \right) \Big|_{\rho_1} \tag{115}$$

Which is proportional to the conserved quantity described previously in (82). As the action is a conserved quantity, we may evaluate the free energy density contribution from this part of the full action at either of the two boundaries. As such, we finally arrive at a formula for the free energy density of the system in terms of the UV free parameters.

$$\mathcal{F} = \lim_{\rho_1 \to \rho_0} e^{2A(\rho)-\chi(\rho)} \left( \frac{1}{4}\partial_\rho A - \frac{1}{2}\partial_\rho \chi \right) \Big|_{\rho=\rho_1} - \lim_{\rho_2 \to \infty} e^{2A(\rho)-\chi(\rho)} \left( \frac{3}{4}\partial_\rho A - \frac{1}{2}\partial_\rho \chi + \mathcal{W}_2 \right) \Big|_{\rho=\rho_2} \tag{116}$$

$$= \lim_{\rho_2 \to \infty} e^{2A_0-\chi_0} \left(3\chi_3\right)\big|_{\rho=\rho_2} - \lim_{\rho_2 \to \infty} e^{2A_0-\chi_0} \left( \frac{1}{2}\phi_1\phi_2 + \frac{2}{3}\varphi_1\varphi_2 + \chi_3 \right) \Big|_{\rho=\rho_2} \tag{117}$$

$$= -\frac{1}{6} e^{2A_0-\chi_0} \left(3\phi_1\phi_2 + 4\varphi_1\varphi_2 - 12\chi_3\right) \tag{118}$$

## 5.3 Numerical Implementation

Here, we will discuss the process of describing the behaviour of the free energy as a function of the parameter space. The first step in doing so is to extract the parameter values $\{\phi_1\,,\ \phi_2,\ \varphi_1,\ \varphi_2,\ \chi_3\}$ corresponding to each individual class of solution, for each starting value of the IR parameters across a range of said values. As before, for each IR expansion, we solve the bulk equations of motion numerically to obtain solutions for $\phi(\rho)$, $\varphi(\rho)$, $\chi(\rho)$, and $A(\rho)$, choosing an appropriate end of space and boundary conditions. As previously mentioned, we must also apply a shift along the radial coordinate in such a way as to set the parameters $\chi_0 = A_0 = 0$, generating a new set of solutions from the old. Finally, we choose some value of the radial coordinate $\rho = \rho_m$ at which we match the value of each solution, as well as its derivatives, to the UV expansions (95)-(98) in order extract $\phi_1$, $\phi_2$, $\varphi_1$, $\varphi_2$, and $\chi_3$.

Before making any determination of the behaviour of the free energy of the system, we made sure to check that the numerical implementation for solving the background equations of motion was consistent. After evolving our solutions towards the region of large $\rho$ in order to obtain the UV parameters, we found that we could indeed use these parameters as boundary conditions in order to solve the equations and find solutions which asymptote back towards the region of small $\rho$ in the IR. Using the same matching process as in the UV, we can recover the IR parameters used to evolve the original solutions.

As noted in the previous section, we will find it convenient to define the following notations

which makes use of a physical rescaling using the parameter $\Lambda$:

$$\hat{\mathcal{F}} = \mathcal{F}\Lambda^{-3} \tag{119}$$

$$\hat{\phi_1} = \phi_1\Lambda^{-1} \tag{120}$$

$$\hat{\phi_2} = \phi_1\Lambda^{-2} \tag{121}$$

$$\hat{\varphi_1} = \varphi_1\Lambda^{-1} \tag{122}$$

$$\hat{\varphi_2} = \varphi_2\Lambda^{-2} \tag{123}$$

$$\hat{\chi_3} = \chi_3\Lambda^{-3}, \tag{124}$$

Such that our analysis is conducted in terms of dimensionless and thus invariant physical quantities, allowing as to appropriately compare the different classes of solution

## 5.4 IR Conformal/Domain wall Backgrounds

We will present here the result of the numerical analysis, in which we derived the relationship between the free energy density $\mathcal{F}$ as a function of the IR deformation parameters $\{\phi_I, \varphi_I\}$, corresponding to the operator with dimension $\Delta = \frac{3+\sqrt{33}}{2}$. Beginning by looking at just the IR-conformal solutions, we note that we have not applied any normalisation using the aforementioned scale setting procedure, as the integral which defines the quantity $\Lambda$ diverges close to the IR fixed point. We will however, reintroduce it when comparing solutions later.

As mentioned previously, it is understood that because of the tendency of the solutions to approach the unstable Englert vacuum, the relationship between the IR parameters is constrained as

$$\frac{\varphi_I}{\phi_I} < 1 - \frac{\log(1+\sqrt{2})}{\log(\frac{1+\sqrt{5}}{2})}. \tag{125}$$

Outside of this constraint, our choice of starting values for these parameters is arbitrary. For ease of selecting values to construct solutions, we set $\varphi_I = -1$ and vary $\phi_I$ between $0 < \phi_I < 1 - \frac{\log(1+\sqrt{2})}{\log(\frac{1+\sqrt{5}}{2})}$. In order to demonstrate the numerical relationship, we tabulate a few

Table 1: Here we provide a small selection of values used in and derived from the numerical analysis. The first two columns show the boundary parameters at the end of space $\rho = \rho_1$ used to evaluate a single given numerical solution. The remaining columns show the results of matching the resulting solution to the UV field expansions at the opposite 'boundary' $\rho = \rho_2$. Our choice of parameterisation in the UV means that all solutions that are IR-conformal will have $\chi_3 = 0$

| $\phi_I$ | $\varphi_I$ | $\phi_1$ | $\phi_2$ | $\varphi_1$ | $\varphi_2$ | $\chi_3$ |
|---|---|---|---|---|---|---|
| 0.8 | $-1$ | 1.026 | $-2.963$ | 1.579 | $-3.170$ | 0 |
| 0.82 | $-1$ | 1.095 | $-3.275$ | 1.638 | $-3.461$ | 0 |
| 0.84 | $-1$ | 1.173 | $-3.643$ | 1.705 | $-3.806$ | 0 |
| 0.86 | $-1$ | 1.259 | $-4.079$ | 1.781 | $-4.217$ | 0 |
| 0.88 | $-1$ | 1.358 | $-4.604$ | 1.869 | $-4.714$ | 0 |
| 0.9 | $-1$ | 1.471 | $-5.245$ | 1.970 | $-5.325$ | 0 |
| 0.92 | $-1$ | 1.603 | $-6.045$ | 2.090 | $-6.090$ | 0 |
| 0.94 | $-1$ | 1.758 | $-7.063$ | 2.232 | $-7.069$ | 0 |
| 0.96 | $-1$ | 1.946 | $-8.397$ | 2.406 | $-8.356$ | 0 |
| 0.98 | $-1$ | 2.177 | $-10.20$ | 2.621 | $-10.11$ | 0 |
| 1. | $-1$ | 2.471 | $-12.76$ | 2.898 | $-12.59$ | 0 |
| 1.02 | $-1$ | 2.861 | $-16.59$ | 3.269 | $-16.34$ | 0 |
| 1.04 | $-1$ | 3.409 | $-22.84$ | 3.794 | $-22.47$ | 0 |
| 1.06 | $-1$ | 4.248 | $-34.38$ | 4.605 | $-33.84$ | 0 |
| 1.08 | $-1$ | 5.741 | $-60.80$ | 6.060 | $-59.96$ | 0 |
| 1.1 | $-1$ | 9.390 | $-157.3$ | 9.650 | $-155.8$ | 0 |

results of the parameter matching procedure and resulting free energy calculation.

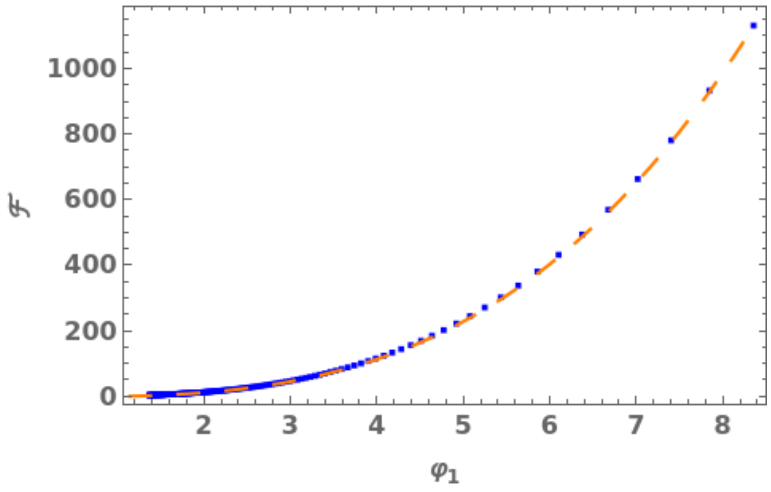


(a)

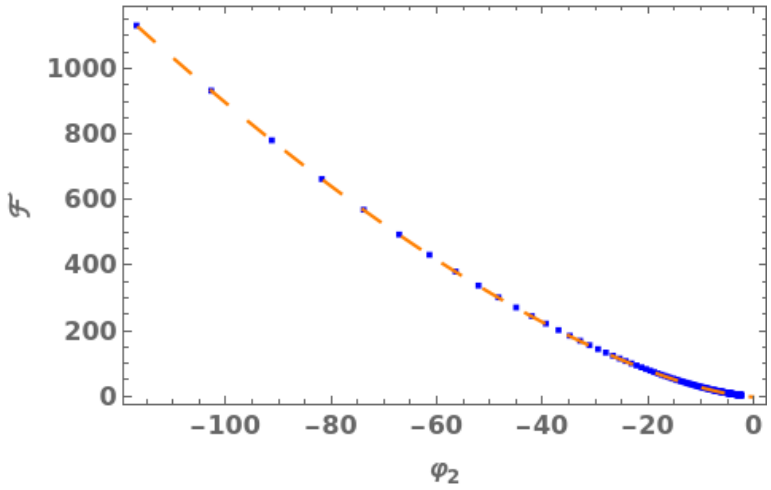


(b)

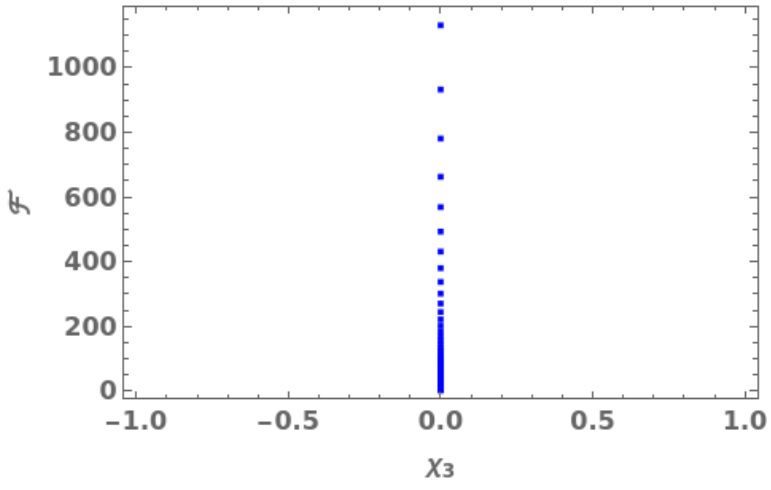


(c)

Figure 5: The free energy density $\hat{\mathcal{F}}$ as a function of the UV deformation parameters $\varphi_1$ (top), $\varphi_2$ (middle), $\chi_3$ (bottom) for the IR-conformal solutions, with the derived power law for the IR conformal solutions superimposed, obtained by varying the IR parameter $\phi_I$. These demonstrate solutions which are asymptotically $AdS$. The first two sets of data can be fitted to the curves $\mathcal{F} = 2\varphi_1^3$ and $\mathcal{F} = (-\varphi_2)^1.5$

The plots above demonstrate the free energy density as a function of the UV deformation parameters $\varphi_1$, $\varphi_2$, and $\chi_3$. Given that the relationship between the free energy and parameters $\phi_1$ and $\phi_2$ is exactly the same as $\varphi_1$ and $\varphi_2$, we neglect to include these results for conciseness. For the plots of $\mathcal{F}$ against $\varphi_1$ and $\varphi_2$, the relationships may be fitted to power laws of the form

$$\mathcal{F} = a\varphi_1^b \tag{126}$$

$$\mathcal{F} = c(-\varphi_2)^d, \tag{127}$$

Where are able to numerically determine that the constants and coefficients $\{a, b, c, d\}$ approach the values $\{2, 3, 1, 1.5\}$. We will use this relationship in the next section to compare with the confining solutions.

## 5.5 Confining/ Soliton Backgrounds

For the solutions that confine, we present a selection of the UV deformation parameters corresponding to a given choice of Integration constant in the IR in table 2. As previously noted, for these solutions each of the parameters is adjusted by the scale setting value $\Lambda$ to facilitate comparison between the confining and IR-conformal solutions.

Table 2: Here we provide a small selection of values used in and derived from the numerical analysis. The first two columns show the boundary parameters at the end of space $\rho = \rho_1$ used to evaluate a single given numerical solution. The remaining columns show the results of matching the resulting solution to the UV field expansions at the opposite 'boundary' $\rho = \rho_2$. These values are representative of solutions which confine as we take $\rho_1 \to 0$

| $\hat{\phi_I}$ | $\hat{\varphi_I}$ | $\hat{\phi_1}$ | $\hat{\phi_2}$ | $\hat{\varphi_1}$ | $\hat{\varphi_2}$ | $\hat{\chi_3}$ | $\Lambda^{-1}$ |
|---|---|---|---|---|---|---|---|
| 0.0000825 | 0.01 | 0.00008441 | −0.00002293 | 0.01023 | −0.002776 | −0.08578 | 7.27562 |
| 0.0000825 | 0.04 | 0.00008480 | −0.00002353 | 0.04098 | −0.01120 | −0.08574 | 7.27653 |
| 0.0000825 | 0.07 | 0.00008567 | −0.00002486 | 0.07196 | −0.02000 | −0.08566 | 7.27852 |
| 0.0000825 | 0.1 | 0.00008704 | −0.00002697 | 0.1033 | −0.02943 | −0.08553 | 7.28159 |
| 0.0000825 | 0.13 | 0.00008893 | −0.00002991 | 0.1353 | −0.03982 | −0.08535 | 7.2857 |
| 0.0000825 | 0.16 | 0.00009139 | −0.00003379 | 0.1680 | −0.05149 | −0.08512 | 7.29084 |
| 0.0000825 | 0.19 | 0.00009446 | −0.00003872 | 0.2018 | −0.06481 | −0.08486 | 7.29696 |
| 0.0000825 | 0.22 | 0.00009823 | −0.00004489 | 0.2367 | −0.08021 | −0.08454 | 7.30402 |
| 0.0000825 | 0.25 | 0.0001028 | −0.00005251 | 0.2732 | −0.09817 | −0.08418 | 7.31196 |
| 0.0000825 | 0.28 | 0.0001082 | −0.00006188 | 0.3114 | −0.1193 | −0.08378 | 7.32071 |
| 0.0000825 | 0.31 | 0.0001147 | −0.00007340 | 0.3517 | −0.1443 | −0.08333 | 7.33021 |
| 0.0000825 | 0.34 | 0.0001224 | −0.00008760 | 0.3946 | −0.1741 | −0.08284 | 7.34035 |
| 0.0000825 | 0.37 | 0.0001317 | −0.0001052 | 0.4404 | −0.2097 | −0.08231 | 7.35103 |
| 0.0000825 | 0.4 | 0.0001427 | −0.0001272 | 0.4899 | −0.2526 | −0.08174 | 7.36214 |
| 0.0000825 | 0.43 | 0.0001560 | −0.0001549 | 0.5436 | −0.3046 | −0.08112 | 7.37352 |
| 0.0000825 | 0.46 | 0.0001721 | −0.0001903 | 0.6025 | −0.3681 | −0.08046 | 7.38503 |
| 0.0000825 | 0.49 | 0.0001918 | −0.0002362 | 0.6676 | −0.4464 | −0.07976 | 7.39646 |

With these confining solutions we also plot the aforementioned power law that characterises the behaviour of the free energy as a function of the parameter space in the IR-conformal background. However, here we will replace the dependent parameters with their dimensionless equivalents detailed in (119)-(124) using the same values of $\Lambda$ used to for scale-setting the confining backgrounds. One can see from the form of the power laws in (126)-(127) that performing this process correctly results in a dimensionless free energy density.

When interpreting the results, it is important to note that we decide to only consider a small section of the entire parameter space of the $\phi_I$ and $\varphi_I$. That is to say, we deliberately set our system to confine much, much before the IR fixed point, at small values by limiting our analysis to only small values of $\phi_I$ and $\varphi_I$. While we found that the trends demonstrated in figures (5)-(7) continue for higher values of the UV parameters, we found that as the solutions that generate them begin to approach the Englert fixed point, the change in $\mathcal{F}$ increases

Table 3: Here we provide a small selection of values used in and derived from the numerical analysis. The first two columns show the boundary parameters at the end of space $\rho = \rho_1$ used to evaluate a single given numerical solution. The remaining columns show the results of matching the resulting solution to the UV field expansions at the opposite 'boundary' $\rho = \rho_2$.

| $\hat{\phi}_I$ | $\hat{\varphi}_I$ | $\hat{\phi}_1$ | $\hat{\phi}_2$ | $\hat{\varphi}_1$ | $\hat{\varphi}_2$ | $\hat{\chi}_3$ | $\Lambda^{-1}$ |
|---|---|---|---|---|---|---|---|
| 0.001 | 0.8 | 0.03067 | −0.1733 | 2.998 | −8.711 | −0.06958 | 7.41969 |
| 0.00100819 | 0.799158 | 0.03039 | −0.1703 | 2.974 | −8.570 | −0.06963 | 7.42029 |
| 0.00101808 | 0.798138 | 0.03005 | −0.1667 | 2.945 | −8.403 | −0.06966 | 7.42102 |
| 0.00103174 | 0.796725 | 0.02959 | −0.1620 | 2.905 | −8.180 | −0.06974 | 7.422 |
| 0.00104907 | 0.794923 | 0.02903 | −0.1563 | 2.857 | −7.909 | −0.06981 | 7.42322 |
| 0.00106996 | 0.792738 | 0.02838 | −0.1497 | 2.800 | −7.599 | −0.06993 | 7.42464 |
| 0.00109425 | 0.790178 | 0.02766 | −0.1426 | 2.737 | −7.259 | −0.07003 | 7.42625 |
| 0.0011218 | 0.787251 | 0.02687 | −0.1351 | 2.668 | −6.898 | −0.07016 | 7.428 |
| 0.00115241 | 0.783965 | 0.02604 | −0.1273 | 2.595 | −6.525 | −0.07031 | 7.42986 |
| 0.00118591 | 0.780328 | 0.02519 | −0.1195 | 2.519 | −6.147 | −0.07046 | 7.4318 |
| 0.00122209 | 0.77635 | 0.02431 | −0.1118 | 2.440 | −5.771 | −0.07064 | 7.43377 |
| 0.00126076 | 0.772039 | 0.02343 | −0.1042 | 2.361 | −5.402 | −0.07081 | 7.43574 |
| 0.00130169 | 0.767404 | 0.02255 | −0.09691 | 2.281 | −5.043 | −0.07101 | 7.43769 |
| 0.00134468 | 0.762452 | 0.02168 | −0.08993 | 2.202 | −4.699 | −0.07121 | 7.43957 |
| 0.00138951 | 0.757192 | 0.02083 | −0.08330 | 2.123 | −4.370 | −0.07143 | 7.44136 |
| 0.00143595 | 0.751632 | 0.02000 | −0.07705 | 2.046 | −4.059 | −0.07165 | 7.44303 |

exponentially when incrementing in equal steps our starting IR value. This makes the process of generating further solutions computationally expensive while reducing the clarity of the results, particularly for the purposes of comparing the two different classes of solution.

Our analysis of the confining background can be divided into two approaches. We began by looking at the behaviour of the free energy as we altered just one of the two free IR parameters, in this case $\varphi_I$.

We also consider cases where our initial choices of $\varphi_I$ and $\phi_I$ are both varied by choosing values that lie along a single RG flow. A few examples of numerical results are shown in Table 3 and Figure 7

Considering each of these results in turn, we learn a number of lessons about the physics of the system we have chosen. Clearly, for the entirety of the parameter space both classes of solutions have a finite free energy density $\hat{\mathcal{F}}$. Furthermore, it is evident that for all choices of parameters which we make, the confining solutions minimise $\hat{\mathcal{F}}$ and so are energetically favoured over the IR conformal solutions. Returning to the language of the dual gauge theory,

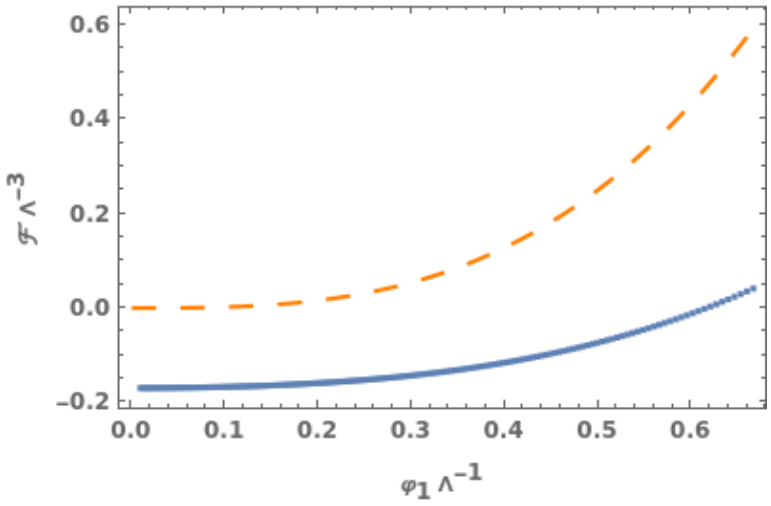


(a) $\hat{\varphi_1}$

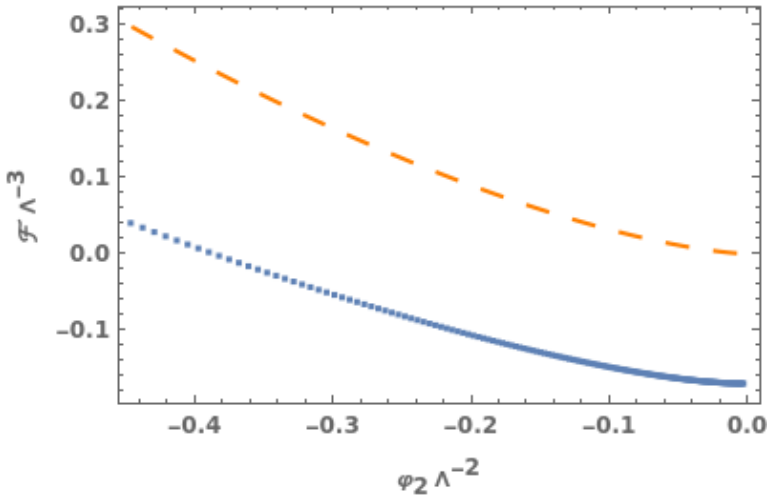


(b) $\hat{\varphi_2}$

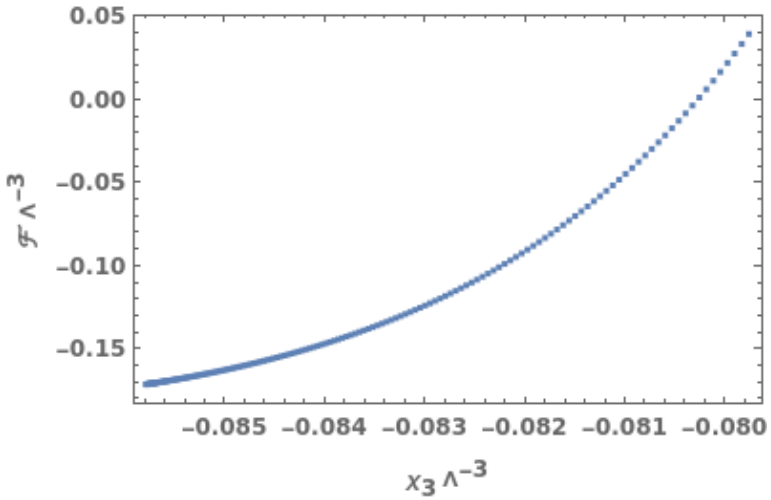


(c) $\hat{\chi_3}$

Figure 6: The free energy density $\hat{\mathcal{F}}$ as a function of the deformation parameters $\hat{\varphi_1}$ (top left), $\hat{\varphi_2}$ (top right), $\hat{\chi_3}$ (bottom) for the confining solutions, with the derived power law for the IR conformal solutions superimposed, obtained by varying the IR parameter $\varphi_I$. These plots demonstrate solutions which confine close to the IR fixed point.

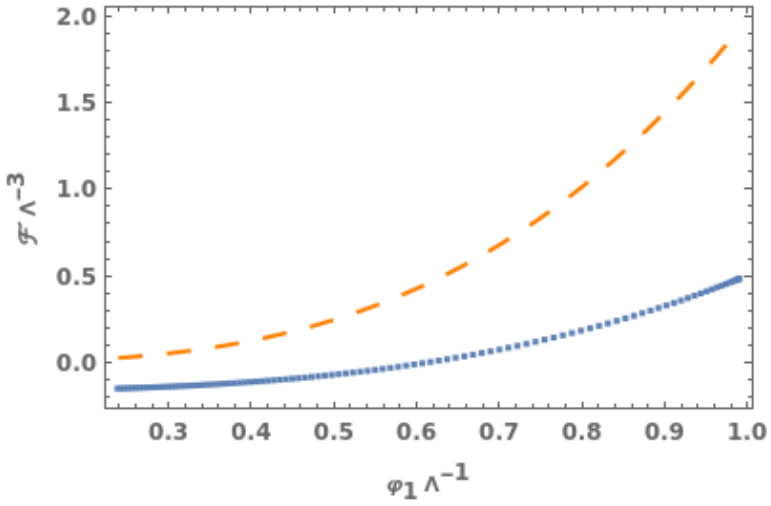


(a) $\hat{\varphi_1}$

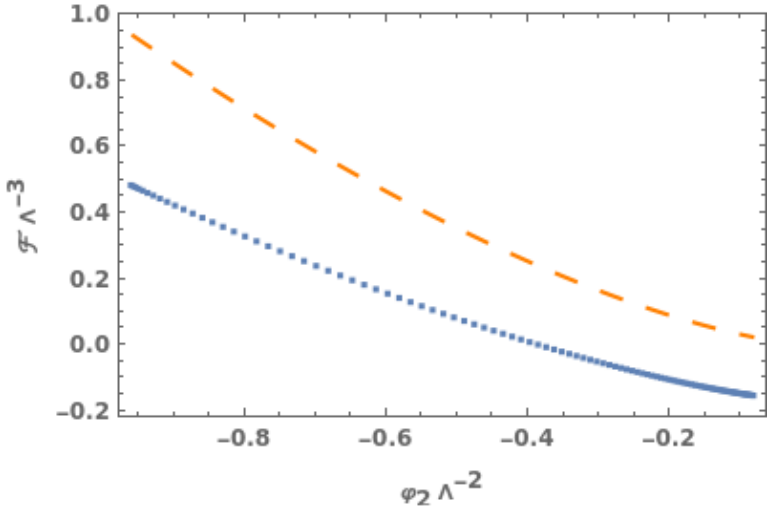


(b) $\hat{\varphi_2}$

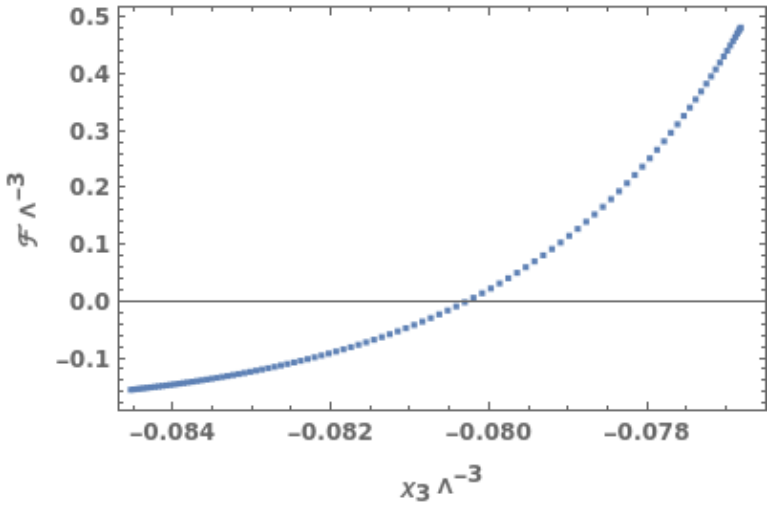


(c) $\hat{\chi_3}$

Figure 7: The free energy density $\hat{\mathcal{F}}$ as a function of the deformation parameters $\hat{\varphi_1}$ (top left), $\hat{\varphi_2}$ (top right), $\hat{\chi_3}$ (bottom) for the confining solutions, with the derived power law for the IR conformal solutions superimposed, obtained by varying the IR parameters $\phi$ and $\varphi_I$ together. These plots demonstrate solutions which confine close to the IR fixed point.

this means that any conformal field theories dual to our choice of gravity background will have couplings that increase without bound at all energy scales, and there is no evidence of a first order phase transition.

# 6 Summary

Starting from a program of research outlined in [16], and starting from a truncation of $AdS \times SE_7$ supergravity defined in [1], we were able to define a new consistent truncation which reduced the number of scalars in the model from 4 to 2 in a "skew-whiffed" model in which supersymmetry was not preserved for most classical solutions. From this newly truncated action, we were able to construct classical equations of motion with a dependence on the scalars $\phi$ and $\varphi$ and the pseudoscalar quantity $\mathcal{A}$.

We next demonstrated the truncation was, in-fact, consistent, by ensuring that our truncations, along with our 'two scalar' equations of motion solved the equations of motions evaluated from a bulk action containing 4 scalars. Once sure of of their consistency, we found that our equations permitted three possible classes of domain wall solution, depending on our choice of boundary conditions. These solutions were found to be in accordance with previous literature discussing the critical points of $\mathcal{N} = 8$ supergravity [1, 55, 57, 53]. Once these critical points had been verified, we constructed near boundary solutions that described the behaviour of our scalar fields in the vicinity of these critical points, in the asymptotic limit of $\rho \to \pm\infty$, where each end of the space represented either the UV or IR conformal limit of a dual quantum field theory. From numerical evaluation of these solutions we were able to find a class of interpolating solutions between the Pope-Warner and Skew-Whiffed critical points, and one single solution which interpolated between the Englert and Skew-Whiffed critical point. When constructing these solutions, we were able to dial the 'IR' parameters such that solutions would approach arbitrarily close to the Englert vacuum and stay there briefly before moving on. However, the instability of the Englert vacuum meant we were unable to construct solutions that flowed directly to it. Each of these interpolating solutions had an important dual field

theory interpretation, representing a renormalisation group flow between the conformal field theories dual to our supergravity fixed points.

We then turned our attention to a slightly altered supergravity compactification in which one of the $AdS_4$ dimensions was compactified on a circle and parameterised by coordinate $\eta$. This space was defined by the condition that the geometry smoothly closed off at the coordinate $\rho = 0$, and became asymptotically $AdS$ as $\rho \to \infty$. As, by definition, the 4 non compact dimensions contains a locally $AdS_3$ subspace, we were able to show via expansion of the appropriate actions that the four-dimensional action is equivalent to the three-dimensional action with the addition of a total derivative term. In other words, we found that there was a global symmetry which meant that solutions to the, comparatively simpler, three-dimensional classical equations of motion, were also solutions to the four-dimensional case.

Consequently, we once again found three classes of solution representing critical points of the potential $V$, these being the *simple confining solutions*. As one might expect, in the limit that the circular dimension becomes large, the confining solutions become asymptotically equivalent to the three classes of $AdS_4$ domain wall solutions. Conversely, in the opposite limit of small $\rho$ we found that the derivatives $\partial_\rho \chi$ and $\partial_\rho A$ now diverge. In any case, we were able to generalise these solutions by expanding for small $\rho$, giving a new set of IR dual expressions (91)-(94) which we used to construct a generalised family of numerical solutions. These numerical solutions were found to exhibit similar behaviour to those which were conformal in the IR, with the exception that these solutions where defined to be dual to QFT's that confine before reaching the IR critical point where the geometry smoothly closes off.

Once we had confirmed the existence of both numerical confining and IR-conformal interpolating solutions, we returned to the classical supergravity action given in (101) in order to begin the process of holographic renormalisation, ultimately culminating in an expression for the free energy density of the system in terms of UV free parameters. After performing an appropriate rescaling and coordinate shift of our numerical solutions, we found, through a process of parameter matching, the behaviour of the free energy density as a function of the UV free parameters. In particular, a comparison of the free energy density of the two classes of

solution demonstrated that solutions of classical supergravity dual to confining quantum field theories are energetically favourable compared to those in which there is a renormalisation group flow to a conformal fixed point in the IR of the theory.

# 7 Conclusion and Outlook

While our results admit a clear interpretation in terms of dual quantum field theories, our results seem to lack many of the more interesting features demonstrated in similar programs of research into other supergravity backgrounds [23, 20, 16], such as tachyonic behaviour and first order phase transitions. Nevertheless, our results remain of some use by clearly demonstrating the free energy behaviour of a two scalar model in this particular supergravity background.

Given more time however there are a number of fascinating and rich avenues of research to explore, using this work in this thesis as a starting point. The most immediate of these would be to begin to explore the scalar mass spectrum of this particular truncation, with the aim of possibly uncovering instabilities that did not clearly present from just an analysis of the free energy.

In terms of additional avenues of research to our original choice of four-dimensional theory, the most simple would be to incorporate additional fields coupled to gravity. This would range in scale of complexity, depending on whether we wished to add just additional scalars, or more complex fermionic and bosonic states. Another simple alteration could consist of altering the sign of one of the terms in our original truncated action, so that our truncated supergravity preserves the supersymmetry of the higher dimensional theory, rather than being 'Skew-Whiffed' as in our model. We may also decide that we wish to explore an entirely different supergravity truncation, as indeed even speaking of just compactifications on $AdS_4$ there are a wealth of possible models. This is especially true when considering circle compactification, where we could explore 'twisted' circle compactifications such as those described in [59]

A subtle but intriguing additional angle for extending this research program lies in our

approach to investigating confinement. Specifically, alternative approaches to those used in this thesis exist using the Klebanov-Strassler and Maldacena-Nunez systems [60, 61]. Each of of these models are specialised constructions that differ from the standard compactifications typically used. In doing so, they allow one to find supergravity backgrounds corresponding to confining gauge theories using more complex geometries.

# A Verifying the consistency of the truncation

A crucial step in the analysis outlined in this thesis is the process of truncating the action outlined in (27) from four scalars to two. In order to ensure the accuracy of any further conclusions we make after this fact, we must first ensure that our choice of truncation is in fact consistent. Initially, these rules were applied to the classical action in order to reduce the number of scalars from four to two. Using this new truncated action, we were able to derive classical equations of motion in scalars $\phi$ and $\varphi$. However, we may also derive equations of motion for four scalars, and truncate these instead.

In order to do this, we start with the classical equations of motion written in terms of the four scalars $\{u, v, h, \chi\}$ given in equations (28)-(31). Substituting into these the series of truncations detailed in equations (32)-(41), we get

$$\begin{aligned}
&\frac{1}{7}\left(-3\partial_\rho A\partial_\rho\phi\tanh(\phi(\rho))+\tanh(\varphi(\rho))\left(3\partial_\rho A\partial_\rho\varphi+\partial_\rho^2\varphi\right)\right.\\
&+\operatorname{sech}(\phi(\rho))\left(-\partial_\rho^2\phi\sinh(\phi(\rho))-\cosh(2\phi(\rho))(-2\cosh(2\varphi(\rho))+\cosh(4\varphi(\rho))+5)\right.\\
&\left.\left.+2\cosh(4\phi(\rho))\sinh^2(\varphi(\rho))+5\cosh(2\varphi(\rho))-1\right)\right)=0,
\end{aligned}\tag{128}$$

$$\begin{aligned}
&-\frac{1}{7\left(e^{2\phi(\rho)}+1\right)\left(e^{2\varphi(\rho)}+1\right)}\left(2e^{\phi(\rho)+\varphi(\rho)}\left(6\sinh(\phi(\rho))\cosh(\varphi(\rho))\left(3\partial_\rho A\partial_\rho\phi+\partial_\rho^2\phi\right)\right.\right.\\
&+8\cosh(\phi(\rho))\sinh(\varphi(\rho))\left(3\partial_\rho A\partial_\rho\varphi+\partial_\rho^2\varphi(\rho)\right)\\
&+\cosh(\varphi(\rho))\left(-\cosh(2\phi(\rho))(-44\cosh(2\varphi(\rho))+\cosh(4\varphi(\rho))+19)\right.\\
&\left.\left.\left.-4\cosh(4\phi(\rho))\sinh^2(\varphi(\rho))(7\cosh(2\varphi(\rho))+3)-30\right)+6\cosh(3\varphi(\rho))\right)\right)=0,
\end{aligned}\tag{129}$$

$$\frac{4e^{2\phi(\rho)}}{\left(e^{2\phi(\rho)}+1\right)^2}\left(3\partial_\rho A\partial_\rho\phi+\partial_\rho^2\phi-2\sinh(3\phi(\rho))\sinh^2(2\varphi(\rho))+8\sinh(\phi(\rho))\cosh^2(y(\rho))\right)=0,\tag{130}$$

$$\frac{8e^{2\varphi(\rho)}}{\sqrt{3}\left(e^{2\varphi(\rho)}+1\right)^2}\left(3\partial_\rho A\partial_\rho\varphi+6\cosh(\phi(\rho))\sinh(2\varphi(\rho))-\cosh(3x(\rho))\sinh(4\varphi(\rho))+\partial_\rho^2\varphi(\rho)\right)=0. \tag{131}$$

From here, substituting out the partial derivatives using the equations (45)-(48) sets the left hand side of these equations to zero, confirming that equivalency of the two sets of equations of motion, and verifying that our truncation rules are consistent.

# References


[1] Jerome P Gauntlett, Seok Kim, Oscar Varela, and Daniel Waldram. Consistent supersymmetric kaluza-klein truncations with massive modes. *Journal of High Energy Physics*, 2009(04):102–102, Apr 2009.

[2] Serguei Chatrchyan et al. Observation of a New Boson at a Mass of 125 GeV with the CMS Experiment at the LHC. *Phys. Lett. B*, 716:30–61, 2012.

[3] Georges Aad et al. Observation of a new particle in the search for the Standard Model Higgs boson with the ATLAS detector at the LHC. *Phys. Lett. B*, 716:1–29, 2012.

[4] Alexander A. Migdal and Mikhail A. Shifman. Dilaton Effective Lagrangian in Gluodynamics. *Phys. Lett. B*, 114:445–449, 1982.

[5] Walter D. Goldberger, Benjamín Grinstein, and Witold Skiba. Distinguishing the higgs boson from the dilaton at the large hadron collider. *Phys. Rev. Lett.*, 100:111802, Mar 2008.

[6] Thomas Appelquist and Yang Bai. Light dilaton in walking gauge theories. *Phys. Rev. D*, 82:071701, Oct 2010.

[7] Deog Ki Hong, Stephen D.H. Hsu, and Francesco Sannino. Composite higgs from higher representations. *Physics Letters B*, 597(1):89–93, September 2004.

[8] P. Hernández-León and L. Merlo. Distinguishing a higgs-like dilaton scenario with a complete bosonic effective field theory basis. *Phys. Rev. D*, 96:075008, Oct 2017.

[9] Zackaria Chacko and Rashmish K. Mishra. Effective theory of a light dilaton. *Phys. Rev. D*, 87.

[10] Edward Witten. Anti de sitter space and holography, 1998.

[11] S.S. Gubser, I.R. Klebanov, and A.M. Polyakov. Gauge theory correlators from non-critical string theory. *Physics Letters B*, 428(1–2):105–114, May 1998.

[12] Juan Maldacena. *International Journal of Theoretical Physics*, 38(4):1113–1133, 1999.

[13] Ofer Aharony, Steven S. Gubser, Juan Maldacena, Hirosi Ooguri, and Yaron Oz. Large n field theories, string theory and gravity. *Physics Reports*, 323(3–4):183–386, January 2000.

[14] Leonard Susskind. The world as a hologram. *Journal of Mathematical Physics*, 36(11):6377–6396, nov 1995.

[15] Zeeya Merali. Collaborative physics: String theory finds a bench mate. *Nature*, 478:302–304, 2011.

[16] Daniel Elander, Maurizio Piai, and John Roughley. Dilatonic states near holographic phase transitions. *Physical Review D*, 103(10), May 2021.

[17] Alex Pomarol, Oriol Pujolas, and Lindber Salas. Holographic conformal transition and light scalars. *Journal of High Energy Physics*, 2019(10), October 2019.

[18] Nick Evans and Kimmo Tuominen. Holographic modelling of a light technidilaton. *Phys. Rev. D*, 87:086003, Apr 2013.

[19] Victor Gorbenko, Slava Rychkov, and Bernardo Zan. Walking, weak first-order transitions, and complex cfts. *Journal of High Energy Physics*, 2018(10), October 2018.

[20] Daniel Elander and Maurizio Piai. Calculable mass hierarchies and a light dilaton from gravity duals. *Physics Letters B*, 772:110–114, September 2017.

[21] Edward Witten. Anti-de sitter space, thermal phase transition, and confinement in gauge theories, 1998.

[22] Daniel Elander, Maurizio Piai, and John Roughley. Probing the holographic dilaton. *Journal of High Energy Physics*, 2020(6), Jun 2020.

[23] Daniel Elander and Maurizio Piai. Light scalars from a compact fifth dimension. *Journal of High Energy Physics*, 2011(1), January 2011.

[24] Victor Gorbenko, Slava Rychkov, and Bernardo Zan. Walking, Weak first-order transitions, and Complex CFTs II. Two-dimensional Potts model at $Q > 4$. *SciPost Phys.*, 5:050, 2018.

[25] Joseph Polchinski. Scale and conformal invariance in quantum field theory. *Nuclear Physics*, 303:226–236, 1988.

[26] Paul Ginsparg. Applied conformal field theory, 1988.

[27] G. C. Wick. Properties of bethe-salpeter wave functions. *Phys. Rev.*, 96:1124–1134, Nov 1954.

[28] James W. York. Role of conformal three-geometry in the dynamics of gravitation. *Phys. Rev. Lett.*, 28:1082–1085, Apr 1972.

[29] G. W. Gibbons and S. W. Hawking. Action integrals and partition functions in quantum gravity. *Phys. Rev. D*, 15:2752–2756, May 1977.

[30] Kostas Skenderis. Lecture notes on holographic renormalization. *Class. Quant. Grav.*, 19:5849–5876, 2002.

[31] Daniel Z. Freedman and Antoine Van Proeyen. *Supergravity*. Cambridge Univ. Press, Cambridge, UK, 5 2012.

[32] Massimo Bianchi, Daniel Z. Freedman, and Kostas Skenderis. Holographic renormalization. *Nucl. Phys. B*, 631:159–194, 2002.

[33] Edward Witten. String theory dynamics in various dimensions. *Nuclear Physics, Section B*, 443:85–126, 3 1995.

[34] Petr Horava and Edward Witten. Heterotic and type i string dynamics from eleven dimensions. *Nuclear Physics B*, 460:506–524, 10 1995.

[35] C. M. Hull and P. K. Townsend. Unity of superstring dualities. *Nuclear Physics, Section B*, 438:109–137, 10 1994.

[36] Peter G. O. Freund and Mark A. Rubin. Dynamics of Dimensional Reduction. *Phys. Lett. B*, 97:233–235, 1980.

[37] Jerome P. Gauntlett and Oscar Varela. Consistent kaluza-klein reductions for general supersymmetric ads solutions. *Physical Review D*, 76(12), December 2007.

[38] M. Cvetič, H. Lü, C.N. Pope, A. Sadrzadeh, and T.A. Tran. Consistent so(6) reduction of type iib supergravity on s. *Nuclear Physics B*, 586(1–2):275–286, October 2000.

[39] Horatiu Nastase, Diana Vaman, and Peter van Nieuwenhuizen. Consistent nonlinear kk reduction of 11d supergravity on ads7×s4 and self-duality in odd dimensions. *Physics Letters B*, 469(1–4):96–102, December 1999.

[40] Horatiu Nastase, Diana Vaman, and Peter van Nieuwenhuizen. Consistency of the ads7×s4 reduction and the origin of self-duality in odd dimensions. *Nuclear Physics B*, 581(1–2):179–239, August 2000.

[41] H. Lü, C.N. Pope, and T.A. Tran. Five-dimensional n=4, su(2)×u(1) gauged supergravity from type iib. *Physics Letters B*, 475(3–4):261–268, March 2000.

[42] B. de Wit and H. Nicolai. The Consistency of the S**7 Truncation in D=11 Supergravity. *Nucl. Phys. B*, 281:211–240, 1987.

[43] M. J. Duff, B. E. W. Nilsson, and C. N. Pope. Kaluza-Klein Supergravity. *Phys. Rept.*, 130:1–142, 1986.

[44] M. Cvetič, H. Lü, and C. N. Pope. Consistent kaluza-klein sphere reductions. *Physical Review D*, 62(6), August 2000.

[45] C N Pope and Kellogg S Stelle. Zilch currents, supersymmetry and Kaluza-Klein consistency. *Phys. Lett. B*, 198:151–155, 1987.

[46] B. de Wit and H. Nicolai. N=8 Supergravity. *Nucl. Phys. B*, 208:323, 1982.

[47] Bernard De Wit and Daniel Z. Freedman. On so(8) extended supergravity. *Nuclear Physics B*, 130:105–113, 11 1977.

[48] B. de Wit and H. Nicolai. Hidden Symmetry in $d = 11$ Supergravity. *Phys. Lett. B*, 155:47–53, 1985.

[49] Z. Bern, J. J. Carrasco, L. J. Dixon, H. Johansson, D. A. Kosower, and R. Roiban. Cancellations beyond finiteness of N=8 supergravity at three loops. *Physical Review Letters*, 98(16), apr 2007.

[50] Z. Bern, J. J. M. Carrasco, L. J. Dixon, H. Johansson, and R. Roiban. Ultraviolet behavior of N=8 supergravity at four loops. *Physical Review Letters*, 103(8), aug 2009.

[51] M. J. Duff, B. E. W. Nilsson, and C. N. Pope. The Criterion for Vacuum Stability in Kaluza-Klein Supergravity. *Phys. Lett. B*, 139:154–158, 1984.

[52] Jerome P. Gauntlett, Julian Sonner, and Toby Wiseman. Quantum criticality and holographic superconductors in m-theory. *Journal of High Energy Physics*, 2010(2), Feb 2010.

[53] Iulia M. Comsa, Moritz Firsching, and Thomas Fischbacher. So(8) supergravity and the magic of machine learning. *Journal of High Energy Physics*, 2019(8), August 2019.

[54] N. P. Warner. Some properties of the scalar potential in gauged supergravity theories. *Nuclear Physics B*, 231:250–268, 1 1984.

[55] N. P. Warner. Some new extrema of the scalar potential of gauged n = 8 supergravity. *Physics Letters B*, 128:169–173, 8 1983.

[56] Krzysztof Pilch and Isaiah Yoo. On perturbative instability of pope-warner solutions on sasaki-einstein manifolds. *Journal of High Energy Physics*, 2013(9), sep 2013.

[57] F. Englert. Spontaneous compactification of eleven-dimensional supergravity. *Physics Letters B*, 119:339–342, 12 1982.

[58] Csaba Csáki, Joshua Erlich, Timothy J. Hollowood, and John Terning. Holographic renormalization group and cosmology in theories with quasilocalized gravity. *Phys. Rev. D*, 63:065019, Feb 2001.

[59] S. Prem Kumar and Ricardo Stuardo. Twisted circle compactification of $\mathcal{N} = 4$ SYM and its Holographic Dual. 5 2024.

[60] Agostino Butti, Mariana Graña, Ruben Minasian, Michela Petrini, and Alberto Zaffaroni. The baryonic branch of klebanov-strassler solution: a supersymmetric family of su(3) structure backgrounds. *Journal of High Energy Physics*, 2005(03):069–069, March 2005.

[61] Juan Martin Maldacena and Carlos Nunez. Towards the large N limit of pure N=1 superYang-Mills. *Phys. Rev. Lett.*, 86:588–591, 2001.